HyUSPRe

Hydrogen **U**nderground **S**torage in **P**orous **Re**servoirs

Experimental data for scaled-down well system on H_2 reactions, effects on casing-cement-rock interfaces, implications for durability and integrity of well systems, and mitigation options for loss of durability and integrity

Prepared by: Jan ter Heege
Vicent Soustelle

TNO Applied Geosciences, Utrecht, The Netherlands

Please cite this report as: Ter Heege, J.H. and Soustelle, V. 2024: Experimental data for scaled-down well system on H2 reactions, effects on casing-cement-rock interfaces, implications for durability and integrity of well systems, and mitigation options for loss of durability and integrity, H2020 HyUSPRe project report, 47 pp.

The authors would like to thank Eric Craenmehr (TNO) and Raymond Cremers (TNO) for performing the exposure experiments.

This report represents HyUSPRe project deliverable number D5.4

The HyUSPRe consortium

Funded by

Acknowledgement

This project has received funding from the Fuel Cells and Hydrogen 2 Joint Undertaking (now Clean Hydrogen Partnership) under grant agreement No 101006632. This Joint Undertaking receives support from the European Union's Horizon 2020 research and innovation programme, Hydrogen Europe and Hydrogen Europe Research.

Disclaimer

Executive summary

Underground hydrogen storage in porous subsurface reservoirs requires cyclic operations of injection and withdrawal of a hydrogen gas stream. During these operations, the following main processes may affect the durability and integrity of well systems, in particular at interfaces between the steel casing, well cement, and porous reservoir:

(1) changes of stress on the well system and expansion or contraction of casing, cement sheath and reservoir due to cyclic variation in pore pressure, temperature,
(2) changes in chemical environment due to long term exposure of hydrogen gas streams that may change the mechanical properties of well materials, and
(3) degradation of well materials due to microbiological or chemical reactions in the reservoir that may lead to corrosive by-products such as H_2S.

In this study, the effects of H_2 exposure and well pressure cycling were experimentally investigated using a newly developed scaled-down well system. The system consists of a steel casing that is cemented in a hollow porous sandstone sample that can be placed in autoclaves for H_2 exposure and in a triaxial apparatus to perform pressure cycling at pressures, temperatures and stresses representative of porous sandstone reservoirs at depths up to ~2.5 km. Casings were either fully perforated to hydraulically connect casing and sandstone, partially perforated to hydraulically connect casing to the interface between casing and intact cement sheath, or not perforated to prevent hydraulic connection between cemented sandstone and casing. In the experiments, well-cemented, consolidated Rijswijk White sandstone and Bentheim sandstone was tested. Rijswijk White sandstone was exposed to N_2 or H_2 for ~143 days at ~19 MPa and 80°C in autoclaves. The scaled-down well samples were subjected to well pressure cycling (max. pressure difference of 20 MPa and cycles of 1-100 hrs) at axial stresses of 16.6-57.4 MPa, confining stresses of 16.0-40.0 MPa and temperatures of 19-75°C (total experimental duration of 104-842 hrs). Effects of H_2 exposure and well pressure cycling was investigated by analyzing sandstone pore pressure response and injected or produced fluid volumes, and based on a proxy for injectivity and productivity (IP index).

The main experimental observations, implications for underground hydrogen storage and mitigation options for loss of durability and integrity of well systems are:

(1) Effects of sequential H_2 exposure and well pressure cycling on sandstone injectivity and productivity or integrity of the scaled-down well systems are small for stress conditions equivalent to reservoirs up to ~2.5 km depth. It suggest that effects of cyclic H_2 injection and withdrawal on sandstone injectivity and productivity are limited for the type of sandstone and conditions tested in the experiments, unless changes in chemical environment significantly affect sandstone deformation *during* injection and withdrawal.
(2) Prolonged well pressure cycling at reservoir conditions for scaled-down well systems exposed to H_2 shows a small decrease injectivity and productivity likely due to inelastic deformation (compaction) of the sandstone. It suggests formation damage (or hydraulic fracturing) need to be taken into account when determining optimum injection and withdrawal conditions.

(3) Hydraulic connection between casing and sandstone is observed after prologened well pressure cycling for scaled-down well systems with partially perforated casings with intact cement sheath. The connection is likely caused by fracturing of the cement sheath.
(4) Mitigation options for loss of durability and integrity have been discussed, including (i) detailed monitoring of well pressures to detect changes in reservoir injectivity and productivity, (ii) changing the location for injection and withdrawal of the H_2 gas stream in the reservoir by re-perforating wells or drilling new wells, and (iii) perform proper assessment of the status of all (active and decommisioned) wells.

About HyUSPRe

Hydrogen **U**nderground **S**torage in **P**orous **Re**servoirs

The HyUSPRe project researches the feasibility and potential of implementing large-scale underground geological storage for renewable hydrogen in Europe. This includes the identification of suitable porous reservoirs for hydrogen storage and technical and economic assessments of the feasibility of implementing large-scale storage in these reservoirs to support the European energy transition to net zero emissions by 2050. The project will address specific technical issues and risks regarding storage in porous reservoirs and conduct an economic analysis to facilitate the decision-making process regarding the development of a portfolio of potential field pilots. A techno-economic assessment, accompanied by environmental, social, and regulatory perspectives on implementation, will allow for the development of a roadmap for widespread hydrogen storage by 2050, indicating the role of large-scale hydrogen storage in achieving a zero-emissions energy system in the EU by 2050.

This project has two specific objectives. Objective 1 concerns the assessment of the technical feasibility, associated risks, and the potential of large-scale underground hydrogen storage in porous reservoirs for Europe. HyUSPRe will establish the important geochemical, microbiological, flow, and transport processes in porous reservoirs in the presence of hydrogen via a combination of laboratory-scale experiments and integrated modelling; and establish more accurate cost estimates to identify the potential business case for hydrogen storage in porous reservoirs. Suitable storage sites will be identified, and their hydrogen storage potential will be assessed. Objective 2 concerns the development of a roadmap for the deployment of geological hydrogen storage up to 2050. The proximity of storage sites to large renewable energy infrastructure and the amount of renewable energy that can be buffered versus time varying demands will be evaluated. This will form a basis for developing future scenario roadmaps and preparing for demonstrations.

Document information, revision history, approval status

Document information

Title:	Experimental data for scaled-down well system on H2 reactions, effects on casing-cement-rock interfaces, implications for durability and integrity of well systems, and mitigation options for loss of durability and integrity
Lead beneficiary:	TNO
Contributing beneficiaries:	TNO
Due date:	M31 (30.4.2024)
Dissemination level:	Public
Published where:	HyUSPRe website
Recommended citation:	Ter Heege, J.H. and Soustelle, V. 2024: Experimental data for scaled-down well system on H2 reactions, effects on casing-cement-rock interfaces, implications for durability and integrity of well systems, and mitigation options for loss of durability and integrity, H2020 HyUSPRe project report, 47 pp.

Revision history

Version	Name	Delivery date	Summary of changes
V01	Ter Heege, J.	7-6-2024	First draft report for review
V02	Ter Heege, J.	18-6-2024	Final report
V03	Cremer, H.	20-6-2024	Final formatted report

Approval status

Role	Name	Delivery date
Deliverable responsible:	J. ter Heege	7-6-2024
Task leader:	J. ter Heege (V. Soustelle)	10-6-2024
WP leader:	J. ter Heege (V. Soustelle)	10-6-2024
HyUSPRe lead scientist	R. Groenenberg	12-6-2024
HyUSPRe consortium manager:	H. Cremer	20-6-2024

Table of Content

1 Introduction

1.1 Deliverable context

Within the HyUSPRe project the feasibility of large-scale storage of renewable hydrogen in porous reservoirs is investigated, including assessment of technical issues and risks. Research on technical issues and risks focusses on geochemical, microbiological, flow and transport, and geomechanical processes that control the response of the subsurface porous reservoir storage system to cyclic injection and withdrawal of a hydrogen-containing gas stream.`A combination of laboratory-scale experiments and integrated modelling was performed to assess this response. This study focussed is on geomechanical processes, i.e. effects of cyclic injection and withdrawal of a hydrogen-containing gas stream that affect the durability and integrity of well systems and reservoir and seals.

This report describes experiments that have been performed in the task on “Effects of cyclic hydrogen injection and withdrawal on integrity of casing-cement-rock interfaces and options to mitigate loss of well integrity”. This task focusses on the effects of hydrogen and cyclic pressures on reservoir injectivity and productivity and integrity of well systems. Maintaining long term efficient reservoir injectivity and productivity is crucial for the success of underground hydrogen storage. Well systems can be leakage pathways for hydrogen if not properly constructed, or if operations critically affect zonal isolation. New experimental data are presented that analyse the effects of hydrogen and cyclic well pressures on a scaled-down well system consisting of steel casing cemented in hollow cylinders of reservoir sandstone at (downhole) pressure, temperature and stress conditions relevant to porous reservoirs.

1.2 Scientific background

Underground hydrogen storage in porous subsurface reservoirs requires cyclic operations of injection and withdrawal of a hydrogen gas stream. These operations can have three main effects on well systems:

- Cyclic variation in pore pressure, temperature and associated changes of stress on the well system causing the casing, cement sheath, and formation to contract and expand alternately.
- Long term exposure of hydrogen gas streams to well materials may change the mechanical properties of well materials due to reactions with hydrogen.
- Interactions with rock and well materials at the reservoir level such as microbiological or chemical reactions may lead to by-products that enhance degradation or erosion of well materials.

If effects are significant, the durability and integrity of well systems may be jeopardized, potentially affecting the efficiency of operations or leading to higher risks of upward hydrogen migration along wells and costly remediation. It is apparent that these effects arise from the combined response of the storage reservoir, cement sheath and steel casing to cyclic injection and withdrawal of hydrogen gas (Figure 1-1).

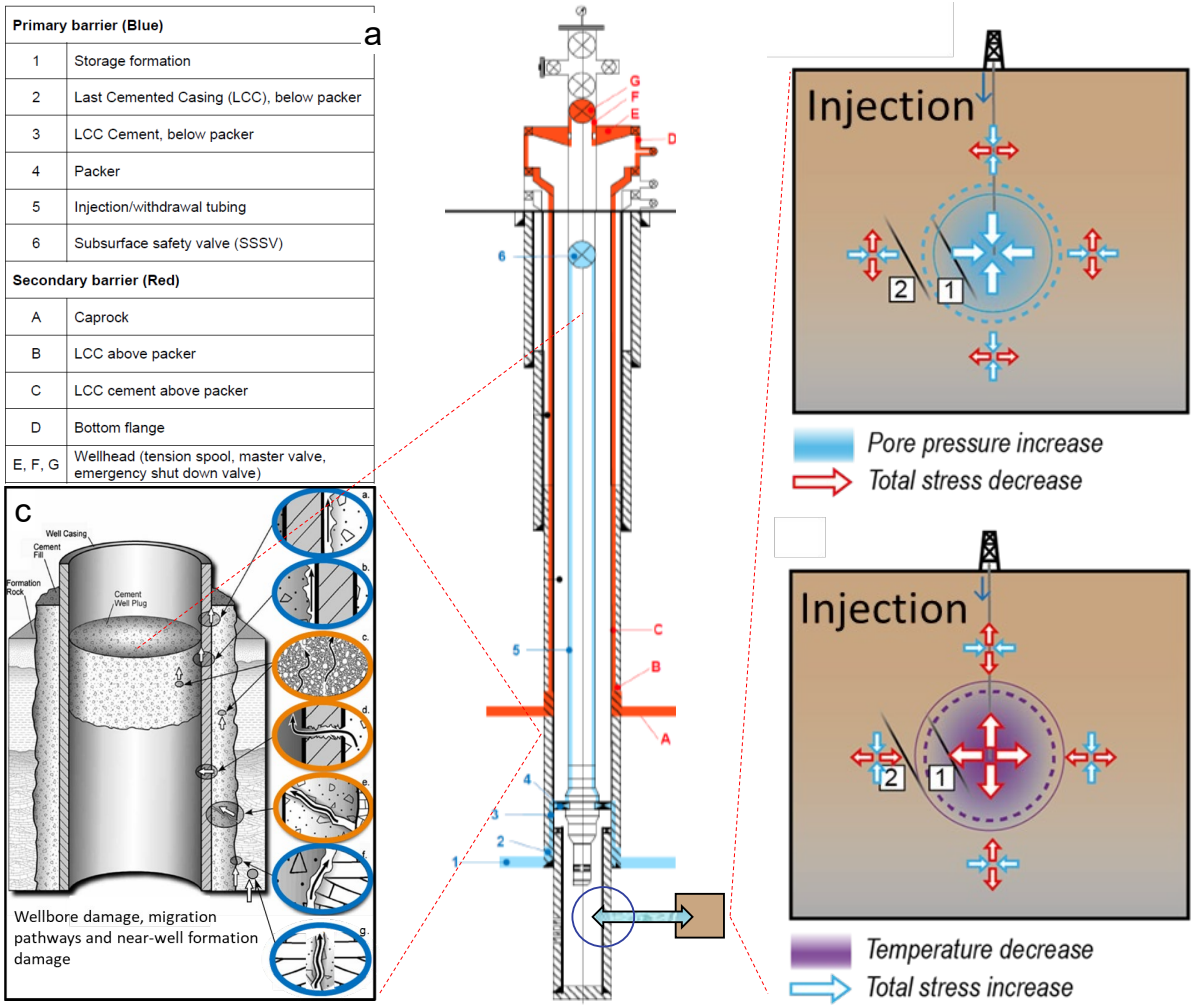

Figure 1-1: Schematic diagram showing key elements of a storage well and effects of hydrogen injection and withdrawal in the (near-well) storage reservoir. (a) Schematic well layout with key barrier elements for a simplified storage well (modified after BVEG 2021). (b) Effects of injection on pore pressure (top) and temperature (bottom) in the reservoir and around faults within (label 1) or outside (label 2) the pressurized or cooled reservoir volume (Buijze et al. 2020). (c) Schematic well section with potential migration pathways caused by wellbore or formation damage (modified after Gasda et al. 2004). Note that an idealized well section is indicated with full cementation of the casing, and that the cement well plug is only relevant for decommissioned wells. The location relevant for the scaled-down well system experiments is indicated by dark blue circles (cf. section 2.2).

Laboratory experiments are crucial for determining effects of H_2 exposure and cyclic stress changes on well systems used for underground hydrogen storage for:

- Identification and description of key controlling processes.
- Determination of critical conditions for loss of performance or elevated risks.
- Quantification of material properties and providing input parameters for models.

Most studies that experimentally investigate the effect of H_2 exposure and cyclic stress changes focus on determining mechanical properties of individual components of well systems, mainly casing steel, well cement, or reservoir rock (Naderloo et al. 2023; Nasiri et al. 2023; Dabbaghi et al. 2024; Ugarte et al. 2024, see also Corina et al. 2022; 2023 and references therein). Some studies focus on casing-cement interaction under different (cyclic) loading conditions (Skorpa et al. 2018; Stormont et al. 2018; Moghadam et al. 2022). Few studies have investigated the combined effects of H_2 exposure and cyclic pore pressure on the durability and integrity of well systems under pressure, stress and temperature conditions relevant for underground hydrogen storage.

In an accompanying study, Corina et al. (2022) outlined some main risks associated with the durability, integrity and efficiency of porous reservoir storage systems under cyclic hydrogen injection and withdrawal. In this outline, two risks focus on well systems, related to (1) reduced injectivity and productivity of hydrogen gas and (2) loss of well integrity and hydrogen leakage along wells. In this study, processes underpinning these two risks were experimentally investigated using a newly developed scaled-down well system for conditions relevant to porous sandstone hydrogen storage reservoirs at depths.

2 Experimental methods

Long term cyclic fluid injection/withdrawal experiments were performed using a newly developed scaled-down well system setup (SDW) to determine (1) the integrity of casing-cement-reservoir system and (2) changes in reservoir injectivity and productivity. The SDW consists of a steel casing that is cemented in a hollow porous sandstone reservoir sample. The setup can be viewed as an scaled-down analogue of a cemented (perforated) well section at reservoir level (Figure 1-1). Different experiments explore the effects of N_2 and H_2 exposure, and casing expansion/contraction by limiting casing perforations. Tests were performed at pressures, temperatures and stresses representative of porous sandstone reservoirs at different depths (up to ~2.5 km depth). Two types of sandstone reservoirs were tested as well as different connectivity between well and reservoir as controlled by casing perforations.

2.1 Sample material

Samples consist of a inner steel cylinder (“casing”), a hollow cylinder of porous sandstone rock, and class G between casing and rock (Figure 2-1). Experiments were performed both with a perforated and intact casing. Perforated casings were prepared by drilling 6 mm diameter holes at 4 diametrically/diagonally opposite locations halfway the casing length using a metal drill.
Rijswijk White (RW) or Bentheim Sandstone (BH) were used for the sandstone reservoir. Samples of Rijswijk White sandstone were drilled from larger blocks using a diamond drill with an inner diameter of 107 mm. A central hole was drilled in the cylindrical samples of the sandstone rock using a diamond drill with an outer diameter of 43 mm, and the samples were trimmed and polished to ~110 mm length using a polishing machine with rotating diamond-coated polishing teeth. The origine of Rijswijk White sandstone is unknown (i.e. the name refers to the Rijswijk Centre of Sustainable Geo-energy (RCSG) where the large sandstone blocks were stored. Properties of the sandstone, such as porosity and permeability, were not determined in this study. Cylindrical samples of Bentheim sandstone (Gildehaus variant) were obtained from Romberg near Bad Bentheim (provided by Natursteinwerk Monser GmbH). Properties of this sandstone have been determined elsewhere (e.g., Dubelaar and Nijland, 2015).

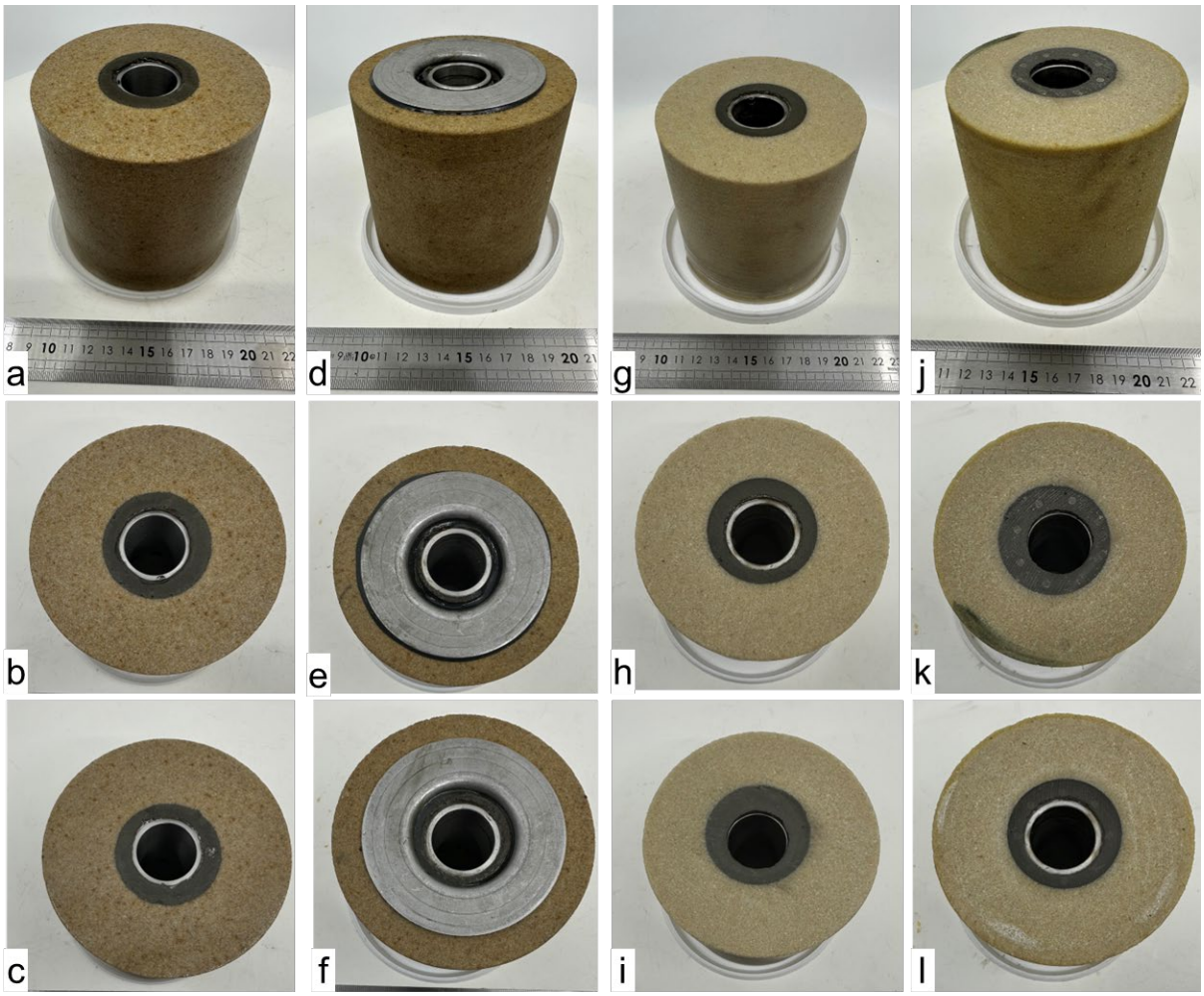

Figure 2-1. Samples with cement sheath between a "casing" and porous sandstone rock. (a, b, c) RW005 (H_2 exposed) before triaxial test. (d, e, f) RW005 (H_2 exposed) with flange after triaxial test. (g, h, i) BH007 (no perforations, no exposure) before triaxial test. (j, k, l) BH007 after triaxial test (no perforations, no exposure). Note the circular impressions in the cement caused by fluid access ports in the sealing rins rings. See appendix A for more samples photos.

Table 2-1. Sample material characteristics. *D*- diameter, *L*- length (subscripts *c*-casing, *s*-cement sheath, *r*- rock, *o*- outer, *i*- inner), *M_r (sat.)*- mass of saturated sandstone sample, *P_{cur}*- curing pressure, *T*- curing temperature, *t_{cur}*- curing time. Note that experiment SDW001 is not included in this report as it was a pilot experiment to test cement sheath properties using a different setup (developed and tested in a different project).

experiment	exposure	casing			cement sheath			hollow rock or outer steel				cement curing		
_sample		D_{co} [mm]	D_{ci} [mm]	L_c [mm]	D_{so} [mm]	D_{si} [mm]	L_s [mm]	D_{ro} [mm]	D_{ri} [mm]	L_r [mm]	M_r (sat.) [g]	P_{cur} [MPa]	T_{cur} [°C]	t_{cur} [days]
SDW002_RW006	no	28.0	25.0	100.0	*44*	28.0	100.0	*104*	*44*	102	-	ambient	80	3
SDW003_RW004	N_2	28.0	25.0	100.0	44.0	28.0	102.2	103.7	44.0	102.2	1917.9	ambient	80	3
SDW005_RW005	H_2	28.0	25.0	100.0	43.6	28.0	102.7	104.0	43.6	102.7	1962.1	ambient	80	3
SDW004_BH006	no	28.0	25.0	100.0	*44*	28.0	103.3	100.4	*44*	103.3	1736.8	ambient	80	5
SDW006_BH007	no	28.0	25.0	100.0	*44*	28.0	104.4	100.3	*44*	104.4	1823.2	ambient	80	5

Class G cement was prepared following practices as outlined in API (2010). Cement is inserted between the casing and rock by placing the rock and casing in a PVC mold and injecting cement through 10 mm diameter PFTE tubes using a manual pump. For the perforated casings, 4 NBR rubber plugs were placed in the casing holes to prevent cement from flowing into the casing. The sample mold was placed in a water bath for 3-5 days at 80°C to cure the cement. After curing, the sample ends were trimmed to 102-105 mm, and polished again. In experiments SDW003_RW004 (N_2 exposure) and SDW005_RW005 (H_2 exposure), part of the top and bottom of the cement-rock interface was drilled after exposure and a steel flange was glued on the sample ends using epoxy to prevent crossflow between the sandstone and cement sheath at the top and bottom of the sample.
Samples were saturated with brine and stored in brine. The brine consisted of 162.6 g/l NaCl, 2.9 g/l KCl, and 40.4 g/l $CaCl_2$. Concentrations of these salts were similar to those used for cement tests in Corina et al. 2023, but $MgCl_2$ and limewater was not used to prevent precipitation of $Mg(OH)_2$ or $Ca(OH)_2$ and prevent alteration of the sandstone rock due to interaction with high pH brine. It does mean leaching of the cement may occur during storage of samples in brine.

2.2 Experimental setup

A scaled-down well system (SDW) was used to perform injection/withdrawal experiments at pressure, temperature and stress conditions equivalent to conditions up to 2.5 km depth (Figure 2-2). Experiments were performed by placing SDW samples in a triaxial deformation apparatus (Figure 2-2a, e). Samples consisting of a central casing cemented in a hollow sample of porous sandstone were sealed against upper and lower sealing rings and pistons with fluid access ports (Figure 2-2b, d). Casings were either intact, perforated through casing alone (intact cement), or perforated through both casing and cement (Table 2-2). Prior to testing, (1) upper and lower sealing rings and pistons with sealing O-rings were inserted in/on top of the casing-cement-sandstone sample, (2) bands of XNBR jacket were placed around the sandstone and sealing ring ends, (3) a transparent polyolefine heat shrink tube (protective jacket) was placed around sandstone and XNBR bands, (4) an XNBR sealing jacket was placed around sample and pistons, and (5) the sealing jacket was sealed against the O-rings in piston grooves using metal wire tourniquet (Figure 2-2b, c). The protective jacket material is added to prevent puncturing of the sealing jacket at high pressure difference between pore (P_p) and confining (P_c) fluids due to small irregularities at the top or bottom of the sample. O-rings between the upper and lower piston and sealing jacket, and between the lower piston and base seal the well fluid from the confining medium. Additional O-rings are placed between the pistons and sealing rings to prevent fluid migration along the piston-sealing rings interfaces. Other seals are part of the triaxial pressure cell (maximum P_c = 40 MPa in the experiments). A ring of fluid ports around the casing ensures uniform distribution of fluid around the top and bottom of the cement sheath (see impressions in Figure 2-2j-l). Well pressures (P_w) were cyclically varied and the resulting pressure in the sandstone and/or at the cement sheath was monitored at specific confining pressures (P_c), axial stresses (σ_a) and temperatures (T_j) conditions (Figure 2-2d). These conditions were systematically varied to pressures, temperatures and stresses equivalent to conditions at different depths (up to 2.5 km).

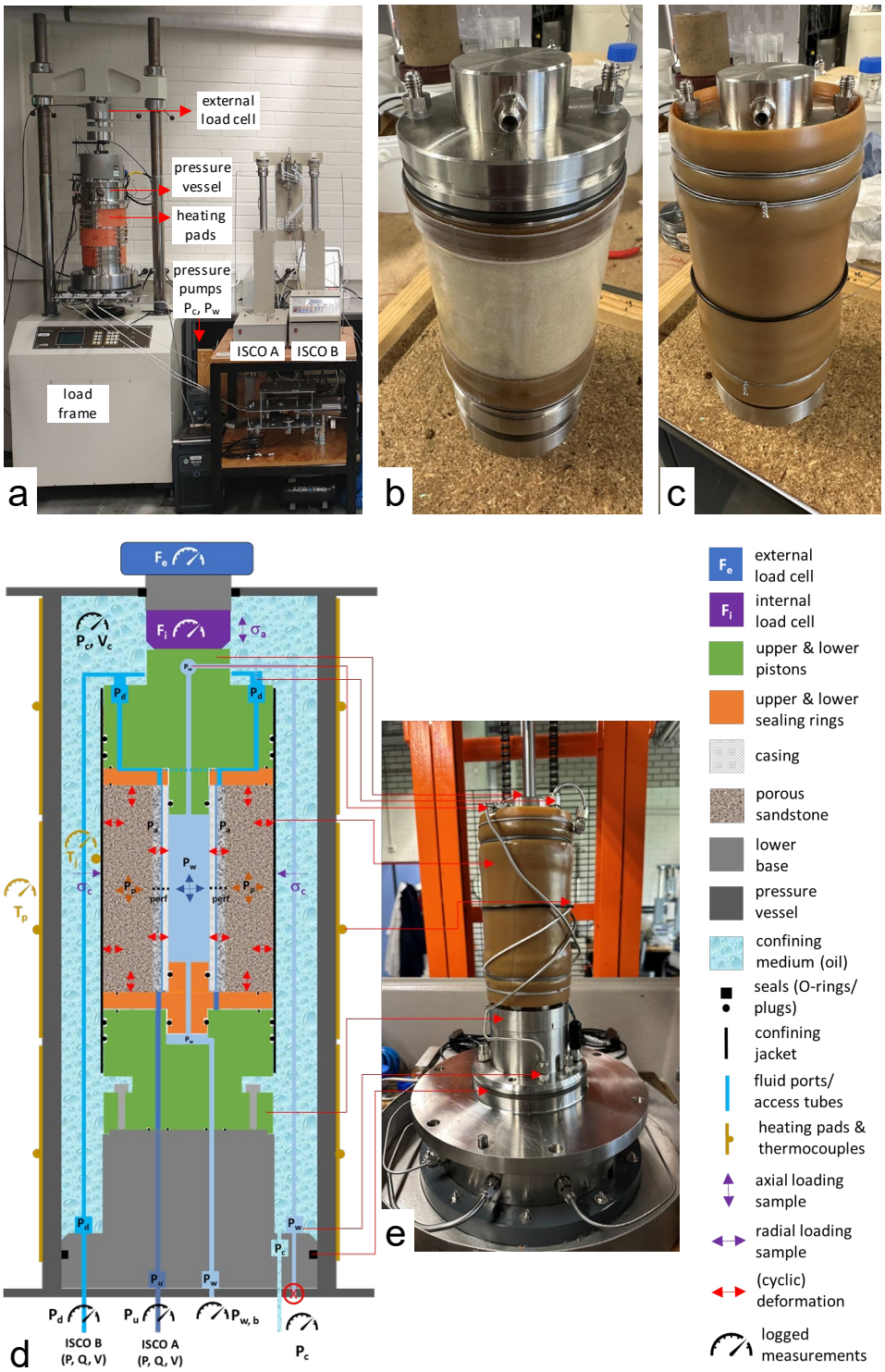

Figure 2-2. Scaled-down well system (SDW) used in triaxial experiments. (a) Triaxial apparatus and pressure pumps. (b, c) Sample SDW006_BH007 with pistons, sealing rings and O-rings, protective jackets (b) and sealing jackets (c). (d) Schematic diagram of setup showing most important components, conditions, and logged measurements. (e) Sample mounted on lower base of triaxial vessel. See legend for symbols and components, and text for further explanation.

Table 2-2. Samples used in different experiments with exposure characteristics and casing setup. *P_{exp}*- gas pressure in autoclaves, *T_{exp}*- autoclave temperature, *t_{exp}*- exposure duraction, *t_{stor}*- storage duration, *perfs./flange*- type of perforations and presence flange (cf. Figure 2-1e, f), *cas*- perfs. throught casing alone, *cas+cem*- perfs. throught casing and cement.

experiment	sample	exposure				storage	perfs./flange
		gas	P_{exp} [MPa]	T_{exp} [°C]	t_{exp} [days]	t_{stor} [days]	-
SDW002	RW006	-	-	-	-	146	cas+cem/no
SDW003	RW004	N_2	19.1	80	144	15	cas+cem/yes
SDW005	RW005	H_2	18.8	80	143	43	cas+cem/yes
SDW004	BH006	-	-	-	-	11	casing/no
SDW006	BH007	-	-	-	-	22	no/no

Exposure of the samples to N_2 and H_2 is done in two 1.6 L stainless steel (316Ti / 1.4571) autoclaves (Premex). Fitted heaters (Premex) around the autoclave are used to heat the autoclaves with temperatures controlled with a thermocouple. A compressor designed for explosive gasses (Booster DLE 30 1-2 by Maximator) is used to generate the high-pressure values of hydrogen.

2.3 Testing procedure

Samples were stored in brine for different duration prior to exposure or testing (Table 2-2). Exposure of samples RW004 and RW005 to N_2 and H_2 was done in parallel in two autoclaves. Samples were submersed in brine with N_2 or H_2 as gas headspace above the samples, and exposed for ~143 days at ~19 MPa and 80°C (RW004, RW005).

The setups were mounted in a triaxial pressure vessel to apply and monitor upstream pressure (P_u, bottom sample/cement sheath), downstream pressure (P_d, top sample/cement sheath), well pressure (P_w), confining pressures (P_c), axial stresses (σ_a) and temperatures (T_j) (Figure 2-2). Julabo Thermal H10 heating bath oil (polydimethylsiloxaan silicone oil) was used as confining oil. Confining pressure (i.e. pressure of oil confining medium) was controlled by a syringe pump. Axial stress (i.e. force exerted by the upper piston) was controlled by movement of a lower ram in the load frame that pushes the setup against a fixed crosshead with internal and external load cells and upper pistons (Figure 2-2e). Upstream, downstream and well/pore pressure were controlled independently by two pressure pumps (ISCO 260D, labelled ISCO A and B) and/or a 200 cc syringe pressure pump (GDS instruments). Temperature was applied by externally heating the pressure vessel using heating pads. Confining pressure, axial stress, well/pore pressure and temperature can be imposed so that the stress state and pressure/temperature conditions of the samples is equivalent to horizontal and vertical stress conditions of wells at depth.

Well pressures were cyclically varied from hydrostatic to low pressures at different rates (max. 1.0 MPa/min) and the resulting (downstream) pressure in the sandstone and/or at the cement sheath was measured as well as the injected/withdrawn fluid volume. Downstream pressure response and injected/withdrawn fluid volume during well pressure cycles was measured for well pressures, confining pressures, axial stresses (σ_a) and temperatures (T_j) equivalent to conditions at different depths. Multiple test stages were performed to systematically apply

equivalent conditions of increasing depths (up to 2.5 km), followed by decreasing depths (down to ~1.0 km). In the stages simulating increasing depths, confining and applied stress were increased first, followed by increase in temperature to disentangle stress and thermal effects on injection and withdrawal. In subsequent stages simulating decreasing depths, stress and temperature were decreased simultaneously (Table 2-3). Typically, tests started with increasing confining pressure to ~1 MPa to initiate a small isotropic stress around the sample and test sealing of sample against the confining oil. Subsequently, the sample was docked against the upper piston using a low displacement rate of the loading ram (~0.5 mm/min), and a small axial stress was applied (below ~0.6 MPa). The confining pressure was increased at ~0.5 MPa/min to ~16.0 MPa in most experiments (except SDW002), and test time is set to zero for plotting and data analysis. The well pressure (~0.5 MPa/min), confining pressure (~0.5 MPa/min) and differential stress (~0.2 MPa/min) were then gradually increased to equivalent conditions of 1.0-2.5 km depth.

A hydrostatic gradient of ~10 MPa/km well pressure, a gradient of horizontal stress of ~16 MPa/km for confining stress, a gradient of vertical stress of ~22 MPa/km for axial stress and a geothermal gradient of ~30°C/km for temperature were assumed to determine equivalent conditions at different depths (i.e. mimicking a normal faulting stress regime with $S_v > S_h$). Cycling of well (and pore pressure of the sandstone) was performed at each loading step (typically 1-5 < P_w < 10-25 MPa with $P_w < P_c$ and ΔP_w depending on stress conditions, cf. Table 2-2). Well pressure cycles typically include (1) a decrease of P_w from hydrostatic pressure to 1 or 5 MPa in 20 minutes, (2) an increase of P_w to hydrostatic pressure in 20 minutes, and (3) a constant P_w for 20 minutes. In experiment SDW006_BH007 the duration of these steps was increased to 200 and 2000 minutes to test the effect of injection/withdrawal rate. After reaching equivalent conditions of 2.5 km depth, temperature was slowly raised to 75°C (~5°C/hr). Different numbers of pressure cycles were performed before decreasing confining stress, axial stress and temperature in multiple stages.

Table 2-3 (next page). Experimental conditions and IP index during well pressure cycles. *time*- start to end of pressure cycling stage (test time), σ_a- axial stress (σ_1, equivalent to S_v), σ_c- confining stress ($\sigma_2 = \sigma_3$, equivalent to S_h), T_j- temperature, P_w- well pressure steps in cycle, t_c- duration of pressure steps in cycle, *IP index*- injectivity/productivity proxy with minimum and maximum values during injection and production of fluid (see section 2.6 for details). Equivalent reservoir conditions as indicated in section 2.3. Only experimental conditions during well pressure cycling are indicated.

experiment	time	σ_a	σ_c	T_j	P_w	t_c	IP index ($Q/\Delta P_w$)				remarks
sample					cycles	cycles	prod_min	prod_max	inj_min	inj_max	(analogue with reservoir
exposure	[hr]	[MPa]	[MPa]	[°C]	[MPa]	[min]		[$m^3.s^{-1}.Pa^{-1}$]			conditions)
SDW002							**2.3E-16**	**3.5E-16**	**4.5E-17**	**3.0E-16**	**min./max. values entire test**
RW006	47.1 - 64.1	48.1	40.0	19.3	25-5-25	20-20-20	2.3E-16	3.5E-16	4.5E-17	2.5E-16	stress conditions to ~2.0-2.5 km
no exposure	79.5 - 95.0	48.1	40.0	19.9	25-5-25	20-20-20	2.7E-16	2.8E-16	2.9E-16	3.0E-16	stress conditions to ~2.0-2.5 km
SDW003							**2.2E-16**	**3.8E-16**	**1.9E-16**	**3.5E-16**	**min./max. values entire test**
RW004	2.9 - 7.8	22.0	16.0	20.4	10-5-10	20-20-20	3.1E-16	3.3E-16	2.1E-16	2.2E-16	stress conditions ~1.0 km
N_2 exposure	8.0 - 12.8	30.0	24.0	20.4	10-5-10	20-20-20	3.2E-16	3.7E-16	2.0E-16	2.0E-16	stress conditions ~1.5 km
	13.0 - 17.8	38.0	32.0	20.7	10-5-10	20-20-20	3.0E-16	3.8E-16	-	-	stress conditions ~2.0 km
	18.1 - 22.7	46.0	40.0	20.1	10-5-10	20-20-20	3.1E-16	3.5E-16	1.9E-16	2.0E-16	larger S_1
	24.0 - 30.7	46.0	40.0	20.1	25-5-25	20-20-20	2.6E-16	2.7E-16	2.6E-16	2.6E-16	increasing cycling pressure
	30.9 - 49.8	50.0	40.0	20.1	25-5-25	20-20-20	2.7E-16	2.7E-16	2.6E-16	2.8E-16	larger S_1
	50.7 - 118.1	55.0	40.0	20.1	25-5-25	20-20-20	2.5E-16	2.7E-16	2.6E-16	2.9E-16	stress conditions ~2.5 km
	125.0 - 143.4	55.0	40.0	50.0	25-5-25	20-20-20	2.3E-16	2.9E-16	2.7E-16	3.3E-16	higher temperature (T eq. ~1.5 km)
	145.4 - 156.1	55.0	40.0	45 - 75	25-5-25	20-20-20	3.4E-16	3.7E-16	3.4E-16	3.5E-16	increasing temp. (T eq. ~2.5 km)
	156.1 - 188.1	55.0	40.0	75 - 30	25-5-25	20-20-20	3.4E-16	3.6E-16	3.4E-16	3.5E-16	decreasing temperature
SDW005							**2.7E-16**	**5.4E-16**	**2.7E-16**	**4.9E-16**	**min./max. values entire test**
RW005	3.8 - 4.5	16.6	16.0	21.0	10-1-10	20-20-20	5.4E-16	5.4E-16	4.9E-16	4.9E-16	initial conditions
H_2 exposure	5.9 - 10.5	22.4	16.0	21.0	10-1-10	20-20-20	4.8E-16	5.3E-16	4.4E-16	4.6E-16	stress conditions ~1.0 km
	11.5 - 15.5	33.6	24.0	21.1	10-1-10	20-20-20	4.2E-16	4.3E-16	3.9E-16	4.0E-16	stress conditions ~1.5 km
	16.9 - 20.5	44.8	32.0	20.9	10-1-10	20-20-20	3.9E-16	4.0E-16	3.8E-16	3.8E-16	stress conditions ~2.0 km
	23.4 - 23.9	56.0	40.0	20.8	10-1-10	20-20-20	4.0E-16	4.0E-16	-	-	stress conditions ~2.5 km
	24.4 - 28.1	56.0	40.0	20.7	25-5-25	20-20-20	2.8E-16	2.8E-16	2.8E-16	2.8E-16	stress conditions ~2.5 km
	28.4 - 45.2	56.0	40.0	22 - 75	25-5-25	20-20-20	2.8E-16	3.2E-16	2.8E-16	3.1E-16	increasing temperature
	45.4 - 218.1	56.0	40.0	75.0	25-5-25	20-20-20	3.4E-16	3.6E-16	3.4E-16	3.5E-16	higher temperature (eq. 2.5 km)
SDW004							**9.6E-17**	**3.3E-16**	**6.8E-17**	**3.8E-16**	**min./max. values entire test**
BH006	0.9 - 1.9	16.7	16.0	20.6	10-5-10	20-20-20	-	-	6.8E-17	2.5E-16	initial conditions
no exposure	4.6 - 46.9	22.9	16.0	20.5	10-5-10	20-20-20	9.6E-17	3.3E-16	1.2E-16	3.8E-16	stress conditions ~1.0 km
	49.8 - 56.0	34.4	24.0	20.9	15-5-15	20-20-20	1.7E-16	2.5E-16	1.7E-16	2.4E-16	stress conditions ~1.5 km
	57.4 - 61.0	45.9	32.0	20.8	15-5-15	20-20-20	1.9E-16	1.9E-16	1.9E-16	2.1E-16	stress conditions ~2.0 km
	61.4 - 72.0	57.3	40.0	20.8	15-5-15	20-20-20	2.0E-16	2.0E-16	2.0E-16	2.0E-16	stress conditions ~2.5 km
	72.4 - 97.2	57.3	40.0	20.8	25-5-25	20-20-20	1.4E-16	1.9E-16	1.5E-16	1.8E-16	increasing cycling pressure
	97.4 - 100.1	57.3	40.0	21 - 50	25-5-25	20-20-20	1.7E-16	1.9E-16	1.5E-16	1.5E-16	increasing temperature
	100.4 - 161.0	57.3	40.0	50.0	25-5-25	20-20-20	1.8E-16	2.0E-16	1.6E-16	1.9E-16	higher temperature (T eq. ~1.5 km)
	161.4 - 164.1	57.3	40.0	52 - 75	25-5-25	20-20-20	2.0E-16	2.1E-16	1.6E-16	1.7E-16	increasing temperature
	164.4 - 172.0	57.3	40.0	75.1	25-5-25	20-20-20	2.0E-16	2.2E-16	1.8E-16	1.9E-16	higher temperature (T eq. ~2.5 km)
	173.3 - 175.0	57.3	40.0	70.0	25-5-25	20-20-20	2.0E-16	2.0E-16	1.8E-16	1.9E-16	lower temperature
	176.4 - 178.0	57.3	40.0	65.0	25-5-25	20-20-20	1.9E-16	1.9E-16	1.8E-16	1.8E-16	lower temperature (T eq. ~2.0 km)
	179.4 - 181.0	57.3	40.0	60.0	25-5-25	20-20-20	1.9E-16	1.9E-16	1.8E-16	1.9E-16	lower temperature
	182.4 - 184.0	57.3	40.0	55.0	25-5-25	20-20-20	1.9E-16	1.9E-16	1.8E-16	1.8E-16	lower temperature
	186.4 - 187.1	57.3	40.0	50.0	25-5-25	20-20-20	1.8E-16	1.8E-16	1.8E-16	2.6E-16	lower temperature (T eq. ~1.5 km)
	187.4 - 191.0	57.3	40.0	50 - 41	25-5-25	20-20-20	1.8E-16	1.8E-16	1.7E-16	1.8E-16	decreasing temperature
SDW006							**1.2E-16**	**2.2E-16**	**1.6E-16**	**4.7E-16**	**min./max. values entire test**
BH006	1.1 - 25.9	22.4	16.0	21.3	10-1-10	20-20-20	1.2E-16	2.2E-16	1.8E-16	4.7E-16	stress conditions ~1.0 km
no exposure	26.3 - 30.9	25.2	18.0	21.4	10-1-10	20-20-20	1.9E-16	2.0E-16	1.8E-16	1.8E-16	stress conditions ~1.1 km
	31.3 - 36.0	28.0	20.0	21.4	10-1-10	20-20-20	1.9E-16	1.9E-16	1.7E-16	1.8E-16	stress conditions ~1.3 km
	36.3 - 41.0	30.8	22.0	21.3	10-1-10	20-20-20	1.9E-16	1.9E-16	1.7E-16	1.8E-16	stress conditions ~1.4 km
	41.3 - 46.0	33.6	24.0	21.3	10-1-10	20-20-20	1.9E-16	1.9E-16	1.7E-16	1.8E-16	stress conditions ~1.5 km
	46.3 - 51.0	36.4	26.0	21.2	10-1-10	20-20-20	1.9E-16	1.9E-16	1.7E-16	1.7E-16	stress conditions ~1.6 km
	51.3 - 56.0	39.2	28.0	21.2	10-1-10	20-20-20	1.8E-16	1.8E-16	1.7E-16	1.7E-16	stress conditions ~1.8 km
	56.3 - 61.0	42.0	30.0	21.0	10-1-10	20-20-20	1.8E-16	1.8E-16	1.7E-16	1.7E-16	stress conditions ~1.9 km
	61.3 - 66.0	44.8	32.0	21.0	10-1-10	20-20-20	1.8E-16	1.8E-16	1.6E-16	1.7E-16	stress conditions ~2.0 km
	66.3 - 71.0	47.6	34.0	20.9	10-1-10	20-20-20	1.8E-16	1.8E-16	1.6E-16	1.7E-16	stress conditions ~2.1 km
	71.3 - 76.0	50.4	36.0	20.8	10-1-10	20-20-20	1.8E-16	1.8E-16	1.6E-16	1.7E-16	stress conditions ~2.3 km
	76.3 - 81.0	53.2	38.0	20.6	10-1-10	20-20-20	1.8E-16	1.8E-16	1.6E-16	1.7E-16	stress conditions ~2.4 km
	81.3 - 93.8	56.0	40.0	20.7	10-1-10	20-20-20	1.7E-16	1.7E-16	1.6E-16	4.4E-16	stress conditions ~2.5 km
	94.3 - 116.0	56.0	40.0	20.2	25-5-25	20-20-20	1.2E-16	1.3E-16	1.3E-16	1.3E-16	increasing cycling pressure
	120.2 - 144.9	56.0	40.0	25.4	25-5-25	20-20-20	1.3E-16	1.4E-16	1.2E-16	1.3E-16	higher temperature (T eq. ~0.8 km)
	147.2 - 150.9	56.0	40.0	30.4	25-5-25	20-20-20	1.3E-16	1.3E-16	1.2E-16	1.3E-16	higher temperature (T eq. ~1.0 km)
	152.2 - 155.9	56.0	40.0	35.4	25-5-25	20-20-20	1.3E-16	1.3E-16	1.2E-16	1.3E-16	higher temperature (T eq. ~1.2 km)
	157.2 - 160.9	56.0	40.0	40.0	25-5-25	20-20-20	1.3E-16	1.4E-16	1.2E-16	1.3E-16	higher temperature (T eq. ~1.3 km)
	162.2 - 165.9	56.0	40.0	45.0	25-5-25	20-20-20	1.3E-16	1.3E-16	1.2E-16	1.3E-16	higher temperature (T eq. ~1.5 km)
	167.2 - 170.9	56.0	40.0	50.0	25-5-25	20-20-20	1.3E-16	1.4E-16	1.2E-16	4.4E-16	higher temperature (T eq. ~1.7 km)
	173.2 - 176.0	56.0	40.0	55.0	25-5-25	20-20-20	1.3E-16	1.4E-16	1.2E-16	1.3E-16	higher temperature (T eq. ~1.8 km)
	178.2 - 181.1	56.0	40.0	60.0	25-5-25	20-20-20	1.4E-16	1.4E-16	1.2E-16	1.3E-16	higher temperature (T eq. ~2.0 km)
	183.3 - 186.1	56.0	40.0	65.0	25-5-25	20-20-20	1.4E-16	1.4E-16	1.2E-16	1.3E-16	higher temperature (T eq. ~2.2 km)
	188.3 - 191.1	56.0	40.0	70.0	25-5-25	20-20-20	1.4E-16	1.4E-16	1.3E-16	1.3E-16	higher temperature (T eq. ~2.3 km)
	193.4 - 339.1	56.0	40.0	75.0	25-5-25	20-20-20	1.1E-16	1.5E-16	3.1E-17	1.3E-16	higher temperature (T eq. ~2.5 km)
	339.4 - 526.1	56.0	40.0	75.0	25-5-25	200-200-200	8.8E-18	8.8E-18	1.2E-17	1.3E-16	longer cycles
	559.4 - 726.1	56.0	40.0	75.0	25-5-25	2000-2000-2000	4.5E-20	4.5E-20	7.0E-19	6.8E-18	longer cycles
	762.6 - 763.8	56.0	40.0	75.0	25-5-25	20-20-20	8.0E-17	8.0E-17	8.3E-17	8.3E-17	lower temperature (T eq. ~2.5 km)
	765.1 - 766.8	56.0	40.0	70.0	25-5-25	20-20-20	9.2E-17	9.2E-17	8.6E-17	8.6E-17	lower temperature (T eq. ~2.3 km)
	768.1 - 769.8	56.0	40.0	65.0	25-5-25	20-20-20	9.0E-17	9.0E-17	8.9E-17	9.0E-17	lower temperature (T eq. ~2.2 km)
	771.1 - 772.8	56.0	40.0	60.0	25-5-25	20-20-20	8.8E-17	8.8E-17	9.0E-17	9.1E-17	lower temperature (T eq. ~2.0 km)
	774.1 - 775.8	56.0	40.0	55.0	25-5-25	20-20-20	8.4E-17	8.5E-17	9.1E-17	9.1E-17	lower temperature (T eq. ~1.8 km)
	778.1 - 778.8	56.0	40.0	50.0	25-5-25	20-20-20	8.1E-17	8.1E-17	8.5E-17	8.5E-17	lower temperature (T eq. ~1.7 km)
	779.1 - 817.8	56.0	40.0	50-23	25-5-25	20-20-20	6.1E-17	6.1E-17	6.6E-17	8.7E-17	decreasing temperature
	818.1 - 841.8	56-22	40-16	22-21	25-5-25	20-20-20	5.9E-17	6.3E-17	6.4E-17	6.6E-17	decreasing stresses

2.4 Measurement & control

During the experiments, the following parameters are continuously monitored (cf. Figure 2-2):

- Confining pressure (P_c) and volume (V_c) of the oil confining medium are measured and controlled using a 200 cc syringe pressure pump (GDS instruments). P_c is controlled by injecting or withdrawing oil from the triaxial cell. P_c controls the confining stress (minimum principal stress, $\sigma_c = \sigma_3$) on the sample that can be viewed as the equivalent of horizontal stress (S_h) in the subsurface.
- Axial load/force (F_a) is measured, both by an internal (F_i) and external (F_e) load cell. F_a is controlled by movement of the loading ram, pressing the sample against the upper piston and load cell assembly that is fixed in position against the crossbar of the load frame. A balanced ram ensures negligible effect of confining pressure on axial load measurements (i.e. negligible upthrust). Together with σ_c that is isotropic around the sample, F_a controls the axial stress ($\sigma_a = F_a / A_s + \sigma_c$ with A_s the sample area). It determines the main principal stress ($\sigma_a = \sigma_1$) and thereby differential stress on the sample ($\Delta\sigma = \sigma_1 - \sigma_3$).
- Temperature (T_j) is measured by a thermocouple located at the outside of the jacketed sample, fixed at the sample center using a large O-ring. T_j is controlled by heating pads around the triaxial vessel with a PID controller determining power supply to the pads based on readings of thermocouples at the sample (T_j) and pads (T_p).
- Upstream (P_u, V_u, Q_u) and downstream (P_d, V_d, Q_d) pressure, volume and flow rate are measured and controlled by the dual high pressure flow pumps (ISCO 260D). P_u and P_d are also measured by two pressure sensors between the pumps and fluid access ports at the pressure vessel. Upstream pump pressure was cyclically varied to control well pressure and/or pressure at the bottom of the cement sheath. Downstream pressure was monitored at the top of the cement sheath.
- Well pressure and volume (P_w, V_w) is measured and controlled by one of the ISCO pumps or by an additional GDS pump. Cyclic variation of well pressure controlled pore pressure in the sandstone (P_p), depending on casing perforations and/or valves connecting well to bottom sample. P_p varied by injection through perforations at the middle of the casing, by casing expansion (no casing perforations, valves closed), or by connecting well pressure with pressure at the bottom of the sample (valves open). Perforations through the casing alone connect well pressure and casing-cement annulus pressure (P_a). The injected/withdrawn fluid volume at the pump (ΔV_w) was used to calculate the IP index (cf. section 2.6).

All parameters are logged at a frequency of 1 Hz. Data reduction was performed for analysis and calculations by taking average values of parameters over 10 s. intervals.

2.5 Experiments

Two types of experiments were performed to analyze the response of the SDW to cyclic pressure changes of the well, cement-casing interface and/or reservoir sample (Table 2-3). For the first type of experiments, three experiments were performed to compare the effect of exposure and cyclic well pressures on reservoir injectivity and productivity for different exposure conditions. Samples consisted of fully perforated casings cemented in hollow cylinders of Rijswijk White sandstone. Full perforations through casing and cement ensured that casing and sandstone were hydraulically connected. Samples were not exposed or exposed to N_2 or H_2 (SDW002_RW006, SDW003_RW004 and SDW005_RW005, respectively). The different pressure cycling stages during each of the experiments are indicated in Table 2-3.
For the second type of experiments, two different experiments were performed to analyze the effect of cyclic well pressures on the casing-cement-rock system and interfaces. Samples consisted of intact or partly perforated casings cemented in hollow cylinders of Bentheim sandstone. For the sample with an intact casing (SDW004_BH006), there is no hydraulic connection between casing and sandstone or cement sheath. For the sample with a partly perforated casing (SDW006_BH007), the casing is hydraulically connected to the casing-cement interface but not to the sandstone. The different pressure cycling stages during each of the experiments are indicated in Table 2-3.

2.6 Injectivity/productivity and well system durability/integrity analysis

IP index was used as a proxy for injectivity and productivity. IP index is mainly dependent on fluid volume stored in the scaled-down well system and, in case of perforated casings, permeability of the sandstone. High IP index indicate large volume changes are needed to achieve specific change in well pressure during well pressure cycling. IP index is defined in this study as the average flow rate Q to achieve a required change in well pressure ΔP_w for a well pressure cycling step (as measured by the ISCO or GDS well/upstream pressure pumps). IP index can be written as:

$$\text{IP index} = \frac{Q}{\Delta P_w}$$

Per definition IP index is positive for fluid production and negative for fluid injection. For convenience, IP_prod and IP_inj are also used which are absolute (positive) values of IP index for production or injection, respectively (note that in figures with experimental data, IP index is plotted as IP/IP* with IP* = 2.0×10^{-17} arbitrarily chosen for scale). For well pressure cycles with constant duration of cycling steps, Δt and ΔP_w are constant so changes in IP index indicate changes in produced or injected fluid volume ΔV_u required to change the pressure in the cycling step. For a scaled-down well system with a casing that is hydraulically connected to the sandstone, these changes in fluid volume are related to the volume of fluid produced from or injected in the sandstone. Accordingly, IP index is a proxy for injectivity and productivity of the

sandstone. For a scaled-down well system with a casing that is not perforated IP index indicated is a proxy for volume changes by casing expansion or contraction.

IP index is analogous (but not similar) to the injectivity (*I*) or productivity (*J*) index often used for oil & gas wells to express the ability of a reservoir to deliver fluids to the wellbore (Haider 1937). Index *I or J* determines flow rate *Q* from a well for a pressure drawdown ($\Delta P = P_w - P_p$), i.e. $I = Q/\Delta P$. As downstream pressure in the sandstone is undrained (connected to the downstream pressure sensor and pump) and changes during the well pressure cycling in the experiments, pressure difference between the casing and sandstone is not constant during pressure cycling (as is approximately the case for *I* and *J*. The scaled-down setup can also be used to determine *I* or *J* for the same boundary conditions as in wells if downstream pressure (P_p) and well pressure (P_w) are kept constant and flow rate *Q* is measured. This was not attempted in this study as it can lead to very high (potentially unstable) flow rates for permeable sandstone.

3 Experimental results

Two types of experiments were performed. The first type analyzed effects of exposure and cyclic well pressures on sandstone flow properties. The second type analyzed effects of cyclic well pressures (and well expansion) on the integrity of the scaled-down well system. Note that detailed sample photos and figures with data for all experiments can be found in Appendix A and B.

3.1 Effects of H_2 exposure and cyclic well pressures on sandstone flow properties

Effects of H_2 exposure and well pressure cycling on injectivity and productivity were investigated for Rijswijk White sandstone in experiments SDW002 (no exposure, no flange), SDW003 (N_2 exposure, with flange) and SDW005 (H_2 exposure, with flange, Table 2-2). In these experiments the casing was fully perforated, so that the casing is hydraulically connected to the sandstone. Experimental conditions during well pressure cycling stages are indicated in Table 2-3. All pressure cycles involved three steps (1) constant P_w of 10 or 25 MPa for 20 minutes, (2) decreasing P_w to 5 or 1 MPa in 20 minutes, and (3) increasing P_w to 10 or 25 MPa in 20 minutes.

In experiment SDW002 (no exposure, Figure 3-1), the SDW was exposed to stress conditions, equivalent to conditions at ~2.0-2.5 km depth. Temperature was raised to ~75°C at the end of the experiment. Two well pressure cycling stages were performed at these stress conditions (i.e. 25-5-25 MPa steps, 19 and 15 cycles, starting at note 5 and 8, respectively). A failure of the well pressure pump interrupted pressure cycling and logging between the two stages. After failure, the pump configuration was modified, so that well pressure was controlled and only downstream pressure at the bottom of the sample was monitored. The axial stress (48.1 MPa, ~2.2 km eq. depth) was relatively low compared to confining stress (40 MPa, ~2.5 km eq. depth) during the cycles. Well pressure cycling was not performed during temperature increase or decrease. The following key observations can be made for the well pressure cycling stages:

- Response of sandstone pore pressure to well pressure cycles: During the first well pressure cycling stage, downstream pressure at the top of the sample was equal to well pressure, while upstream pressure at the bottom of the sample showed limited response to well pressure changes (Figure 3-1a). During the second well pressure cycling stage, downstream pressure at the bottom of the sandstone sample cyclically changes by ~5 MPa while the average downstream pressure decreases with progressive well pressure cycles. It suggests that well pressure cycling results in a short term effect on sandstone pore pressure as well as longer term pressure equilibration during subsequent cycles (at least locally, at the sample bottom).
- Injected/produced fluid volume: Upstream fluid volume continuously decreases during both well pressure cycling stages (Figure 3-1b), indicating progressive fluid loss from the upstream pump in the system. This fluid loss can have multiple causes, including increased storage of fluid in the system. Upstream volume changes during individual cycles show much less variation during the second well pressure cycling stage compared to the first stage.

- IP index: Except for some outliers, IP_prod shows little variation during the first well pressure cycling stage while IP_inj is decreasing (Figure 3-1b). Both IP_prod and IP_inj show little variation during the second well pressure cycling stage, but values are higher compared to the first stage.

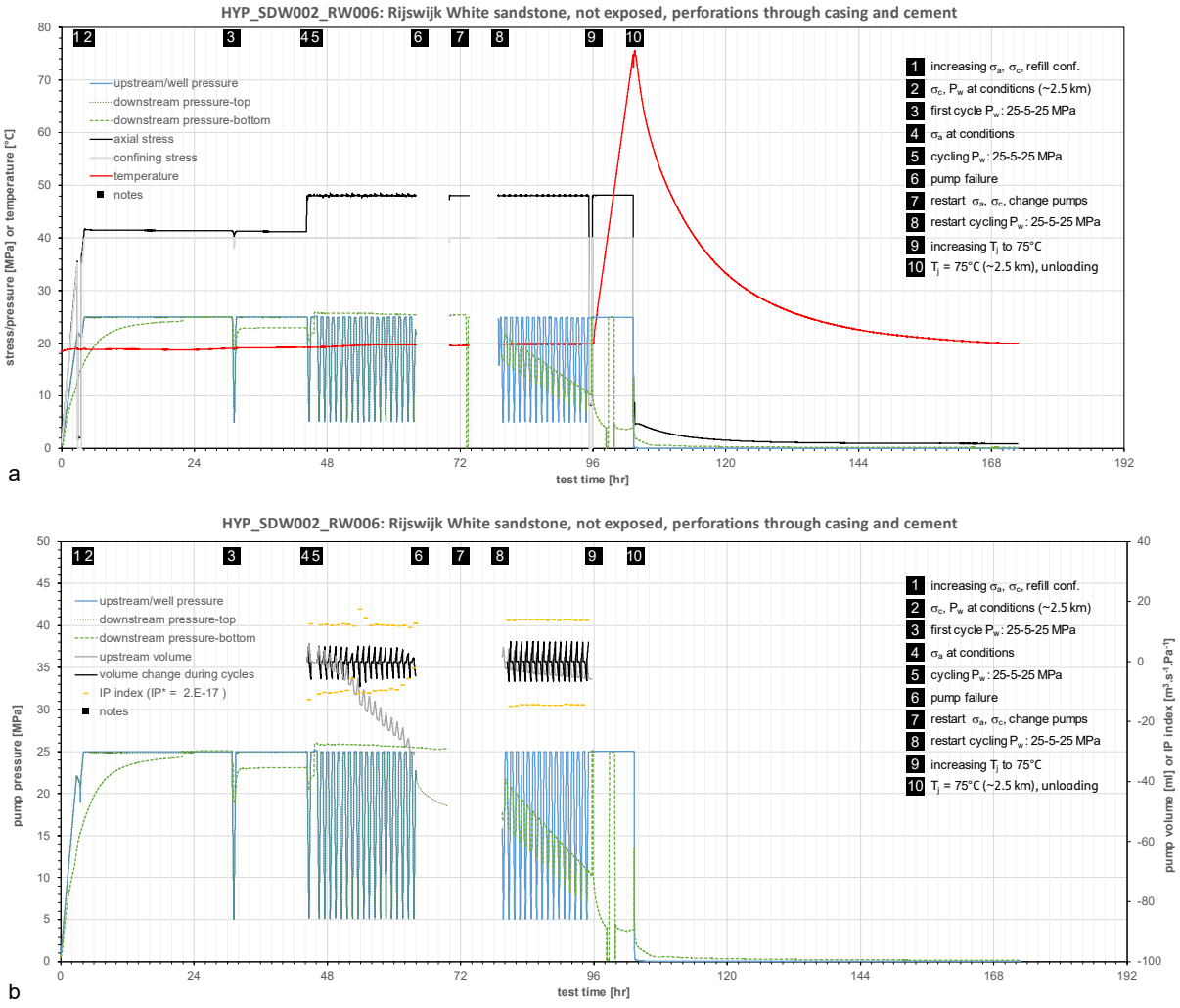

Figure 3-1. Experimental conditions and well pressure cycles for experiment SDW002 on Rijswijk White sandstone (SDW002_RW006, no exposure, tested after cement curing). (a) Axial and confining stress, well, upstream and downstream pressure (as measured by pressure sensors in between pressure pumps and sample), and temperature. (b) well, upstream and downstream pressure and volume (as measured by pressure pumps), and calculated volume changes for each pressure cycle and IP index (injectivity/productivity proxy, cf. section 2.6). Notes of critical experimental steps are also indicated.

In experiment SDW003 (N_2 exposure, Figure 3-2), the SDW was gradually exposed to stress conditions equivalent to conditions at ~1.0, 1.5, 2.0 and 2.5 km equivalent depth. Temperature was raised to ~50 and 75°C in two stages at the end of the experiment. Two well pressure cycling stages were performed (i.e. 19 cycles with 10-5-10 MPa steps and 151 cycles with 25-5-25 MPa steps, starting at note 1 and 3, respectively). The axial stress was relatively low compared to confining stress during the cycles at ~1.0-2.0 km equivalent depth. For the cycles at ~2.5 km equivalent depth, stress conditions matched the overall gradient of ~22 MPa/km and ~16 MPa/km for axial and confining stress, respectively. The following key observations can be made for the well pressure cycling stages:

- Response of sandstone pore pressure to well pressure cycles: During the well pressure cycling stages, downstream pressure at the top of the sample was equal to well pressure, indicating direct pressure communication between casing and sample end (Figure 3-2a).
- Injected/produced fluid volume: Upstream fluid volume continuously decreases during well pressure cycling (Figure 3-2b), indicating progressive fluid loss from the upstream pump. This fluid loss can have multiple causes, including increased storage of fluid in the system. Upstream volume changes during individual cycles mainly show variation when changing maximum well pressures from 10 to 25 MPa, when changing temperature to ~50 and 75°C, and when lowering stresses at the end of the experiment.
- IP index: IP_prod and IP_inj show some variation during the first well pressure cycling stage. IP_prod decreases and IP_inj increases upon changing to the second well pressure cycling stage (Figure 3-2b). Variation in IP_prod and IP_inj is limited during the second cycling stage up to the first heating stage. IP_prod and IP_inj are affected by both heating stages, resulting in higher values at the end of the experiment.

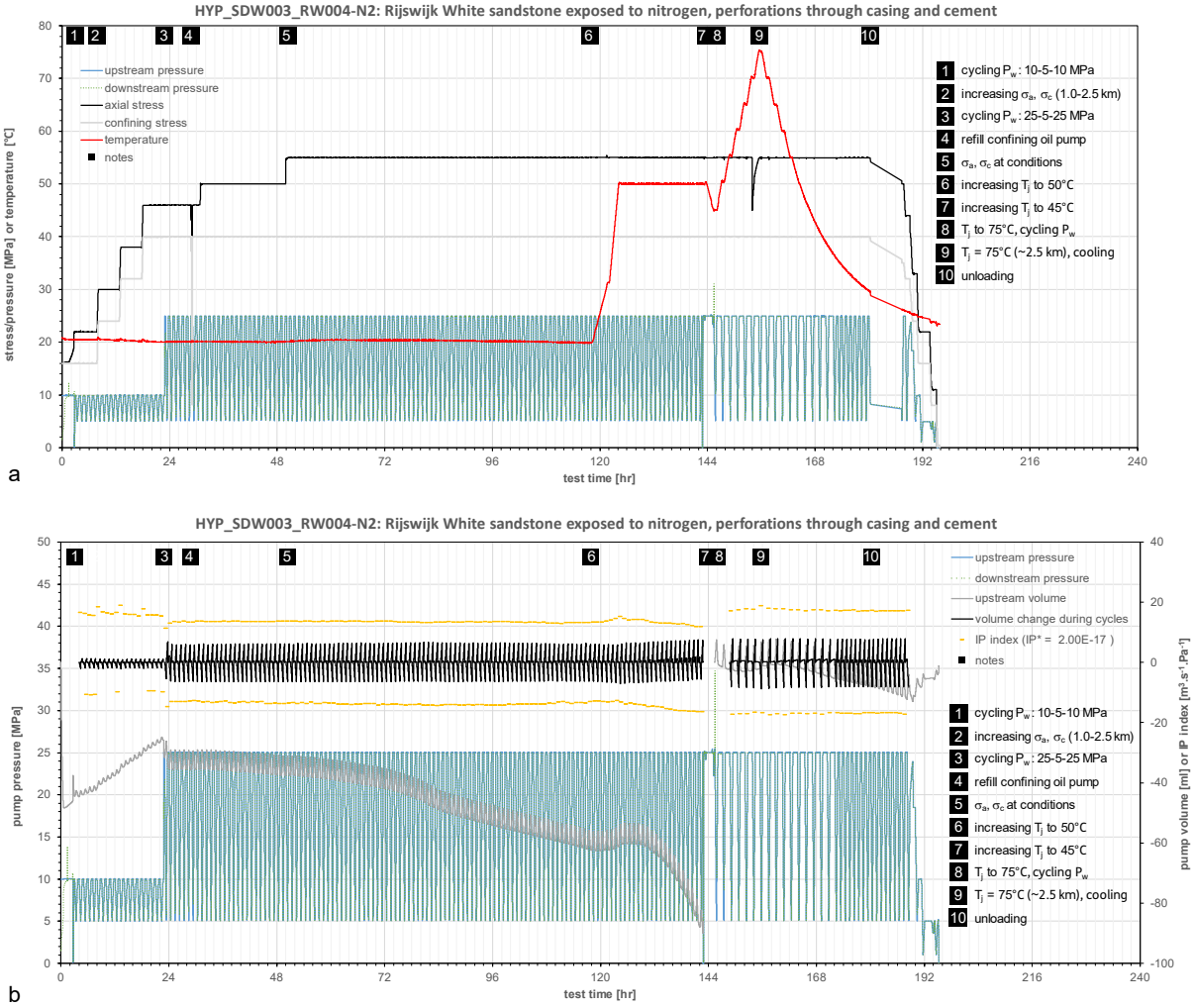

Figure 3-2. Experimental conditions and well pressure cycles for experiment SDW003 on Rijswijk White sandstone (SDW003_RW004, N_2 exposure for ~143 days at ~19 MPa and 80°C). (a) Axial and confining stress, well, upstream and downstream pressure (as measured by pressure sensors in between pressure pumps and sample), and temperature. (b) well, upstream and downstream pressure and volume (as measured by pressure pumps), and calculated volume changes for each pressure cycle and IP index (injectivity/productivity proxy, cf. section 2.6). Notes of critical experimental steps are also indicated.

In experiment SDW005 (H_2 exposure, Figure 3-3), the SDW was gradually exposed to stress conditions equivalent to conditions at ~1.0, 1.5, 2.0 and 2.5 km equivalent depth. Temperature was raised to ~75°C in a single stage. Two well pressure cycling stages were performed (i.e. 20 cycles with 10-5-10 MPa steps and 195 cycles with 25-5-25 MPa steps, starting at note 1 and 2, respectively). Stress and temperature conditions matched the overall gradient of ~22 MPa/km, ~16 MPa/km and ~30°C/km for axial, confining stress and temperature, respectively. A power failure prevented well pressure cycling during lowering of stresses and temperatures at the end of the experiment. The following key observations can be made for the well pressure cycling stages:

- Response of sandstone pore pressure to well pressure cycles: During the well pressure cycling stages, downstream pressure in the sample reached maximum well pressures but not the minimum well pressures (Figure 3-3a). Cycle step (1) with 20 minutes of constant maximum well pressure allowed downstream pressure to equilibrate with well pressure. The immediate change from decreasing to increasing well pressures between cycle step (2) and (3) prevented equilibration of downstream pressure to minimum well pressure. It indicates time-dependent pressure equilibration in the sample, likely controlled by sample permeability. After reaching stress and temperature conditions equivalent to reservoirs at ~2.5 km depth (test time ~48.5 hr), the minimum downstream pressure reached during well pressure cycling gradually increases. It suggests that subsequent cycles result in somewhat slower pressure equilibration (possibly due to reduction in sandstone permeability).
- Injected/produced fluid volume: Upstream fluid volume continuously decreases during well pressure cycling (Figure 3-3b), indicating progressive fluid loss from the upstream pump. This fluid loss can have multiple causes, including increased storage of fluid in the system. Upstream volume changes during individual cycles mainly show significant variation when changing maximum well pressures from 10 to 25 MPa, and minor variation when changing temperature to ~75°C.
- IP index: IP_prod and IP_inj significantly decrease during the first well pressure cycling stage with stresses increasing to ~2.5 km equivalent depth, likely reflecting elastic compaction of sandstone and compression of the casing (Figure 3-3b). Both IP_prod and IP_inj decrease when changing to the second well pressure cycling stage. Subsequent heating to ~75°C results in a ~12 and ~10% increase of IP_prod and IP_inj, respectively. Well pressure cycling at stress and temperature conditions for reservoir sandstones at ~2.5 km equivalent depth resulted in a decrease of IP_prod and IP_inj of ~5 and ~4%, respectively.

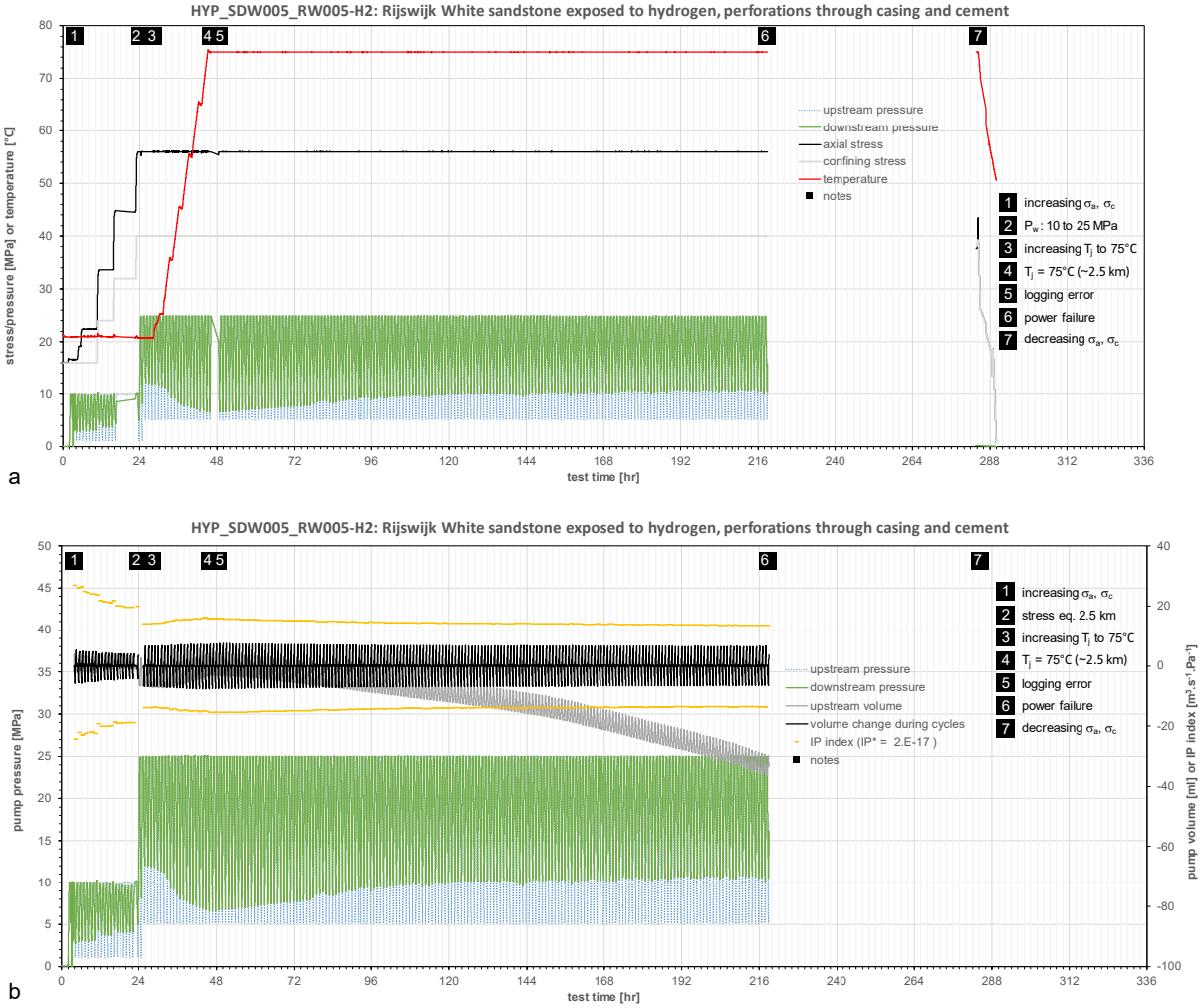

Figure 3-3. Experimental conditions and well pressure cycles for experiment SDW005 on Rijswijk White sandstone (SDW005_RW005, H_2 exposure for ~143 days at ~19 MPa and 80°C). (a) Axial and confining stress, well, upstream and downstream pressure (as measured by pressure sensors in between pressure pumps and sample), and temperature. (b) well, upstream and downstream pressure and volume (as measured by pressure pumps), and calculated volume changes for each pressure cycle and IP index (injectivity/productivity proxy, cf. section 2.6). Notes of critical experimental steps are also indicated.

The effect of H_2 exposure on sandstone injectivity and productivity can be qualitatively evaluated by comparing IP index for experiments SDW002, SDW003 and SDW005 (Table 2-3). For most conditions, maximum and minimum IP_prod is equal or higher than IP_inj. As differences in IP_prod and IP_inj reflect differences in fluid volume required to change the well pressure during cycling, it seems to indicate that fluid withdrawal is easier than fluid injection in the system. It likely reflects that fluid production is aided by higher pressure in the sandstone, while fluid injection needs to work against the higher sandstone pore pressure. Maximum IP_prod and IP_inj for all conditions in the experiments is higher for the H_2 exposed sample (RW005) compared to N_2 (RW003) or not exposed sample (RW006). If compared at the same equivalent depth, IP index is up to a factor ~2 higher for the H_2 exposed sample compared to the N_2 exposed sample. This difference can be due to different injectivity/productivity, but also due to the different well pressure range in the cycles. If IP index from similar well pressure cycles at stress conditions of ~2.5 km equivalent depth are compared, differences are negligible. Another important factor in this comparison is sample variability. Repeated experiments to evaluate reproducibility were not performed in this study. The overall observation is that IP index is comparable when compared at similar stress and well pressure cycling conditions, suggesting limited variability between samples despite different exposure conditions.

3.2 Effects of cyclic well pressures on the integrity of the scaled-down well system

Effects of well pressure cycling on the durability and integrity of the scaled-down well system was investigated for Bentheim sandstone in experiments SDW004 and SDW006. In experiment SDW004 only the casing was perforated, leaving the cement sheath intact and limiting hydraulic connection between the casing and casing-cement interface. In experiment SDW004, the casing was intact, so that hydraulic connection between the casing and cement or sandstone is prevented. Accordingly, effects of well pressure cycling on the cement and sandstone result from casing expansion and contraction alone (as long as the cement sheath is not fractured during experiment SDW004). Experimental conditions during well pressure cycling stages are indicated in Table 2-3. All pressure cycles involved three steps (1) constant P_w of 10 or 25 MPa for 20, 200 or 2000 min., (2) decreasing P_w to 5 or 1 MPa in 20, 200 or 2000 min., and (3) increasing P_w to 10 or 25 MPa in 20, 200 or 2000 min.

In experiment SDW004 (Figure 3-4), the SDW was exposed to stress conditions, equivalent to conditions at ~1.0-2.5 km depth. Temperature was raised in two stages to ~50°C and ~75°C. Three well pressure cycling stages were performed at these stress conditions (i.e. 40 cycles with 10-5-10 MPa steps, 22 cycles with 15-5-15 MPa steps, and 120 cycles with 25-5-25 MPa steps, starting at note 1, 3 and 6, respectively, with 20 min. steps in all stages). Stress and temperature conditions matched the overall gradient of ~22 MPa/km, ~16 MPa/km and ~30°C/km for axial, confining stress and temperature, respectively. The following key observations can be made for the well pressure cycling stages:

- Response of sandstone pore pressure to well pressure cycles: During the first well pressure cycling stage, downstream pressure range at the top of the sample was equal to the well pressure range during cycles (Figure 3-4a). During the second stage, downstream pressure reached maximum well pressures but not the minimum well pressures. During the third stage, the response of downstream pressure to well pressure cycling varied and maximum/minimum well pressure were not reached during most cycles. Towards the end of the experiment, the downstream pressure response to well pressure cycling was comparable to that in experiment SDW005 (Figure 3-3). Marked changes of downstream pressure response occur at test time of ~88 hr, suggesting that the cement sheath no longer prevented hydraulic communication between the casing and sandstone and was likely fractured. It indicates time-dependent pressure equilibration in the sample, possibly controlled by sample permeability and/or cement fracturing. Some of the changes in downstream pressure response to well pressure cycling could result from progressive fracturing of the cement sheath.
- Injected/produced fluid volume: Upstream fluid volume continuously decreases during well pressure cycling (Figure 3-4b), indicating progressive fluid loss from the upstream pump. This fluid loss can have multiple causes, including increased storage of fluid in the system. Upstream volume changes during individual cycles mainly show significant variation when changing maximum well pressures from 10 to 15 MPa and from 15 to 25 MPa. Changes in downstream pressure response to well pressure cycling (test time ~88 hr) is also linked to significant variation in upstream volume changes during cycling.

Significant variation in upstream volume changes is also observed when temperature is changed to ~50°C, to ~75°C and back to ~35°C.

- IP index: IP index is a proxy for injectivity/productivity in the sandstone through (fractured) cement in this experiment (Figure 3-4b). IP_prod and IP_inj show significant variation with changing stress and temperature conditions. Variation in IP index is also linked to changes in the downstream pressure response to well pressure cycling (test time ~88 hr). As discussed above, it could point to fracturing of the cement sheath that affects hydraulic connection between casing and sandstone. During long term well pressure cycling at stress conditions of ~2.5 equivalent depth and temperature of ~50°C, variation in IP_prod and IP_inj is limited.

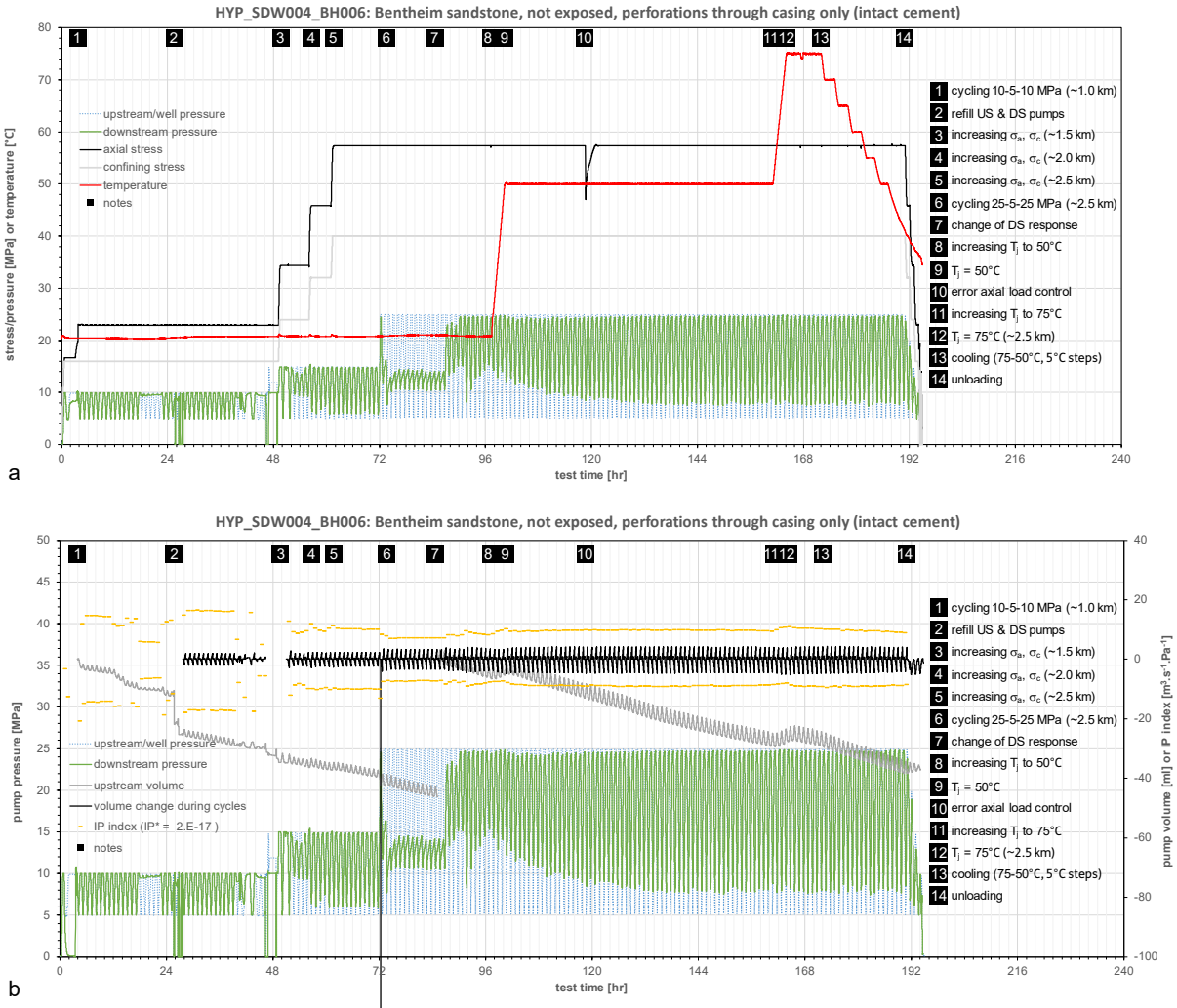

Figure 3-4. Experimental conditions and well pressure cycles for experiment SDW004 on Bentheim sandstone (SDW004_BH006, no exposure, tested after cement curing). (a) Axial and confining stress, well, upstream and downstream pressure (as measured by pressure sensors in between pressure pumps and sample), and temperature. (b) well, upstream and downstream pressure and volume (as measured by pressure pumps), and calculated volume changes for each pressure cycle and IP index (injectivity/productivity proxy, cf. section 2.6). Notes of critical experimental steps are also indicated.

In experiment SDW006 (Figure 3-5), the SDW was exposed to stress conditions, equivalent to conditions at ~1.0-2.5 km depth with increasing equivalent depths in steps of ~1.125 km. Temperature was raised to ~75°C in steps of ~5°C. Five well pressure cycling stages were performed at these stress conditions, i.e. 94 cycles with 10-1-10 MPa steps (20 minute per step, start experiment to note 2), 241 cycles with 25-5-25 MPa steps (20 minute per step, starting at note 2), 24 cycles with 25-5-25 MPa steps (200 minute per step, starting at note 7), 3 cycles with 25-5-25 MPa steps (2000 minute per step, starting at note 9), and 120 cycles with 25-5-25 MPa steps (20 minutes per step, starting at note 10). Stress and temperature conditions matched the overall gradient of ~22 MPa/km, ~16 MPa/km and ~30°C/km for axial, confining stress and temperature, respectively. The following key observations can be made for the well pressure cycling stages:

- Response of sandstone pore pressure to well pressure cycles: As the casing is not perforated SDW006, the response of downstream pressure to well pressure cycling is completely different from the other experiments in this study. Downstream pressure at the top of the sample is varying in response to well pressure cycling, but with with a much smaller pressure range than in the other experiments (Figure 3-5a). The response of downstream pressure is governed by a poro-elastic response to elastic compression and expansion of the SDW resulting from well pressure changes. The increase in maximum well pressure between the first and second cycling stage results in an increase in downstream pressure as compression/expansion of the SDW increases. Most short term changes in downstream pressure ranges are linked to changes in stress and temperature conditions (and associated compression and expansion of the SDW), or linked to manual pressure equilibration in the pumps and/or sandstone (e.g., at test time 313.4 hr). There is also a long term trend of increasing average downstream pressure during the third and fourth cycling stage (starting at test time 339.4 hr). The decrease in downstream pressures in the fifth cycling stage are linked to decrease in temperature and stresses.
- Injected/produced fluid volume: Upstream fluid volume continuously decreases during well pressure cycling (Figure 3-5b), indicating progressive fluid loss from the upstream pump. This fluid loss can have multiple causes, including increased storage of fluid in the system. Upstream volume changes during individual cycles mainly show significant variation when (1) maximum well pressures changed from 10 to 25 MPa (test time 93.7 hr), (2) pressure equilibration was performed (test time 313.4 hr), (3) the duration of cycle steps changed (test time 339.4 hr and 527.2 hr), and (4) temperatures and stresses decreased (test time 763.1 hr).
- IP index: As the casing is not hydraulically connected to the sandstone sample and cement sheath in this experiment (i.e. casing is not perforated), IP index is a proxy for fluid storage in the casing. Well pressure cycling causes elastic casing expansion and contraction (and/or retraction of the sealing pistons to maintain constant axial stress). Casing expansion and contraction is reflected by changes in injected/produced upstream fluid volume for each cycle and related IP index (Figure 2-5b). IP_prod and IP_inj show some variation with changing stress and temperature conditions at the beginning and end of the experiment, which reflects changes in casing stresses and elastic deformation. IP index is lower at the end of the experiment compared to the beginning, suggesting some permanent change of casing fluid storage. Given the

definition of IP index (cf. section 2.6), a linear relation exist between IP index and the duration of steps in well pressure. Accordingly, increasing step duration in the third and fourth cycling stage to 200 and 2000 min. reduces IP index by a factor of 10 and 100, respectively.

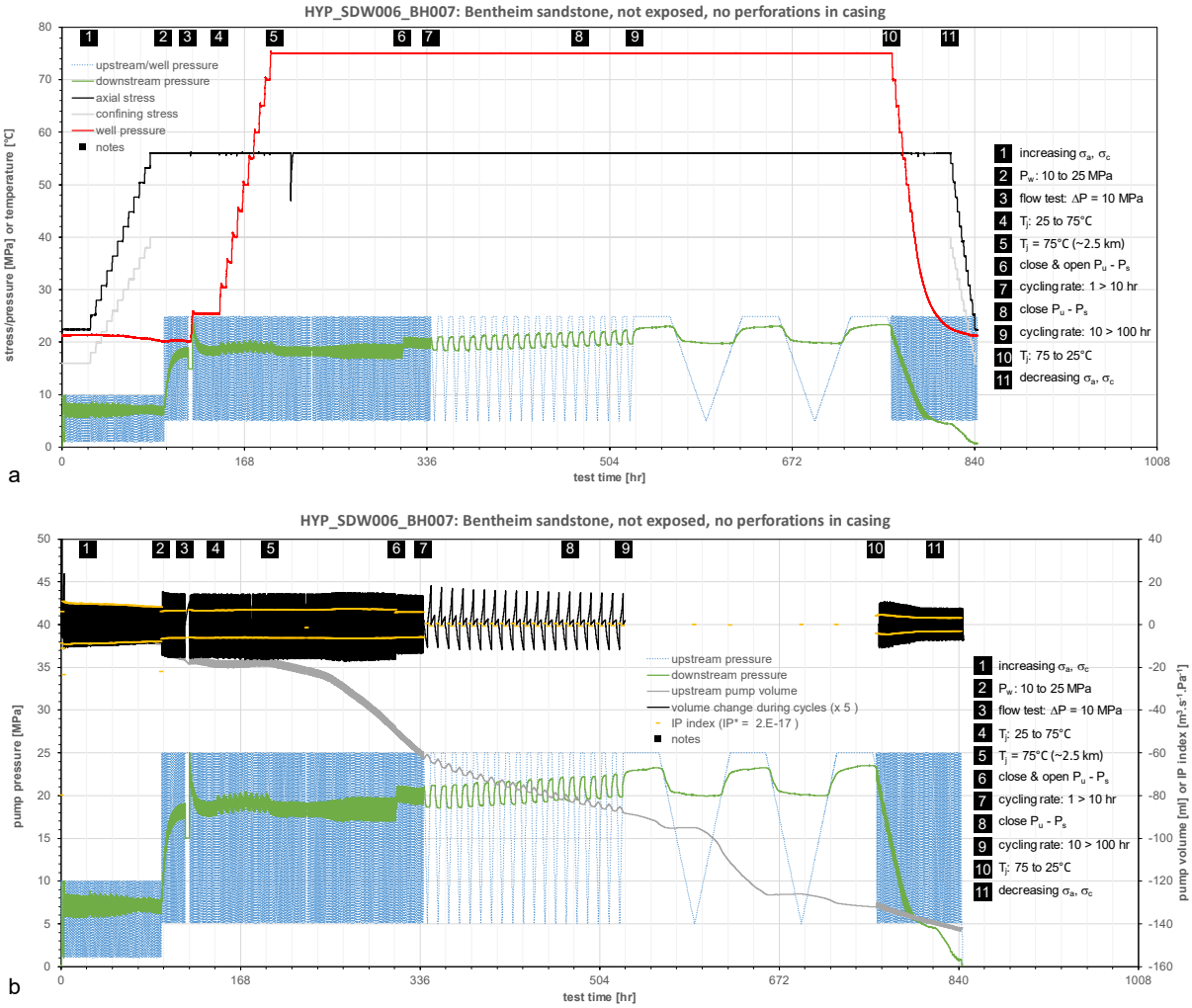

Figure 3-5. Experimental conditions and well pressure cycles for experiment SDW006 on Bentheim sandstone (SDW006_BH007, no exposure, tested after cement curing). (a) Axial and confining stress, well, upstream and downstream pressure (as measured by pressure sensors in between pressure pumps and sample), and temperature. (b) well, upstream and downstream pressure and volume (as measured by pressure pumps), and calculated volume changes for each pressure cycle and IP index (injectivity/productivity proxy, cf. section 2.6). Notes of critical experimental steps are also indicated.

The effect of well pressure cycling on integrity of the scaled-down well system can be evaluated by comparing the response of downstream pressure to well pressure cycling in all experiments (SDW002-SDW006). The integrity of the cement sheath is tested in experiment SDW004. Perforations in sample SDW004_BH006 are limited to the casing, hydraulically connecting the casing to the casing-cement interface but not to the sandstone. The downstream pressure response to well pressure cycling changes during cycling (at test time 87.4) for stress conditions equivalent to ~2.5 km depth. After this change the response is comparable as observed in experiments SDW002, SDW003 and SDW005. It suggests that fracturing of the cement sheath causes hydraulic connection between casing and sandstone.
In experiment SDW006, five long term well pressure cycling stages were performed. No major changes in downstream pressure response to cycling is observed, although there is a long term increase of a average downstream pressure for stress and temperature conditions equivalent to ~2.5 km depth. It may reflect small changes in the system (for example, sandstone compaction or changes in the transfer of elastic casing deformation to cement and sandstone). However, major changes in downstream pressure during cycling that point to loss of integrity of the SDW are not observed.

4 Discussion

4.1 Injectivity and productivity of sandstone storage reservoirs

Effects of H_2 exposure on sandstone injectivity and productivity is evaluated by comparing experiments on scaled-down well systems with fully perforated casing that hydraulically connect the casing to Rijswijk White sandstone (cf. section 3.1). The systems have been subjected to a large number of well pressure cycles (34-215 cycles in experiments running for 104-290 hrs) with pressures cycling between 10 or 25 MPa and 1 or 5 MPa in 40 minutes for samples without exposure (SDW002_RW006), after exposure to N_2 (SDW003_RW003) and after exposure to H_2 (SDW005_RW005). Injectivity and productivity changes are analyzed using pressure changes in the sandstone (downstream), changes in fluid volume during well pressure cycling and IP index. IP index is a proxy for injectivity and productivity that determines the average flow rate needed to change well pressure over fixed time intervals (cf. section 2.6). The key observation from the experiments is that effects of H_2 exposure and well pressure cycling on sandstone injectivity and productivity are small. No major changes in injectivity or productivity are observed, in particular if similar well pressure cycles at stress conditions of ~2.5 km equivalent reservoir depth are compared. A more significant effect is observed if IP index is compared for similar stress and temperature conditions. However, different well pressure ranges in cycles or sample variability may also contribute to different injectivity and productivity. Prolonged well pressure cycling at reservoir conditions for the H_2 exposed sample shows a small decrease in IP index of 4-5%. It suggests cyclic pore pressure may result in small variations in injectivity and productivity after long term cycling, but these observations need to be confirmed in repeated experiments to demonstrate reproducibility of the effect.

Other studies mainly have investigated effects of H_2 exposure and/or cyclic pore pressure variations in triaxial experiments (Schimmel et al. 2021; Naderloo et al. 2023; Dabbaghi et al. 2024). In an accompanying study, Soustelle et al. (2024) performed pore pressure cycling experiments on two different types of sandstones. Core samples representative of deep, relatively hot storage reservoirs and intermediate depth, colder storage reservoirs were tested. Pore pressure cycling was performed at reservoir conditions with cyclic pore pressure changes of ~11 MPa and rate of pressure change of 10 MPa/h. They found small variations (< 10%) in elastic modulus and permeability of the sandstones after 10 pore pressure cycles, and different trends for H_2 exposed sandstones compared to N_2 exposed samples. The largest changes in permeability occurred in the first pore pressure cycle, and permeability decrease seemed to be associated with inelastic strain in the samples. For N_2 exposed sandstone, permeability continues to decrease with smaller changes in subsequent pore pressure cycles. For H_2 exposed sandstones, permeability increases after the initial decrease in the first cycle. The different sandstones and experimental conditions hamper direct comparison with results in this study, but both studies concur that effects of effects of H_2 exposure and pore pressure cycling on sandstone flow properties are small.

Implications for the injectivity and productivity of sandstone storage reservoirs used for underground hydrogen storage can be considered. The experimental results in these studies suggest that effects of cyclic H_2 injection and withdrawal on sandstone injectivity and productivity are limited. Small effects on mechanical and flow properties may be expected (mainly due to inelastic deformation), but these will not likely significantly affect H_2 injection

and withdrawal operations. An important note is that limitations of the experiments need to be taken into account and additional experiments need to support current findings (typically 3 experiments for one type of sandstone at similar conditions) in order to rule out any effects for long term underground hydrogen storage operations (cf. section 4.3).

4.2 Durability and integrity of well systems

Effects of well pressure cycling on integrity of the scaled-down well system is evaluated by analyzing pore pressure changes in the sandstone (downstream) during well pressure cycling in the different experiments. It is assumed that loss of integrity of the system will result in marked changes in sandstone pore pressure changes due to well pressure cycling. For example, loss of integrity can be caused by extensive compaction and associated reduction of sandstone permeability or by development of microannuli along casing-cement or cement-rock interfaces that may cause upward migration of H_2. Besides the systems with fully perforated casing (cf. section 4.1), experiments on scaled-down well systems with no perforations (SDW006_BH007) or partially perforations (SDW004_BH006) and intact cement sheath were performed using Bentheim sandstone as the reservoir sample (cf. section 3.2). The two systems have been subjected to a large number of well pressure cycles (182-454 cycles in experiments running for 195-842 hrs) with pressures cycling between 10 or 25 MPa and 1 or 5 MPa in 40, 400 or 4000 minutes. Due to partial or non-perforated casings, the casing is (initially) not hydraulically connected to the sandstone. The systems investigate the ability of the cement sheath to sustain pressure cycles and the effects of elastic casing expansion or contraction due to pressure cycles, respectively.

The key observation from the experiments is that changes in the sandstone pore pressure response to well pressure cycling are limited if compared at similar experimental conditions. It suggests that loss of system integrity does not occur for scaled-down well systems, even for prolonged well pressure cycling (> 200 cycles with ΔP_w = 20 MPa) at constant stress and temperature conditions. Marked changes in sandstone pore pressure only occur for the scaled-down well system with partial perforations and intact cement sheath that hydraulically connect the casing to the casing-cement interface rather than the sandstone. In that case, the cement-casing interface experiences maximum pressure change during cycling while the cement-rock interface is similar to pore pressure in the sandstone. Accordingly, the cement sheath needs to accommodate the difference between well pressure and sandstone pore pressure that cyclically vary during well pressure cycling. The marked change in sandstone pore pressure response observed in the experiment suggests that the cement sheath cannot sustain these pressure differences for continued well pressure cycling. Likely, the changes in sandstone pore pressure response is due to fracturing of the cement sheath around the casing perforations that causes hydraulic connection between casing and sandstone. This observation shows the limit of cement sheath integrity in this special case and provides data on in situ strength of the cement sheath. However, it is not considered representative for well systems at actual underground hydrogen storage sites, except maybe locally at perforations or poorly cemented well sections.

It is not straightforward to directly transfer the experimental results to assessment of critical conditions for loss of durability or integrity of actual storage wells. The experimental findings do show that these type of well cemented sandstones can sustain long term pressure cycling

without loss of mechanical strength. Therefore, mechanical support of the well system by the storage reservoir is not likely affected by prolonged pressure cycling for these types of sandstone reservoirs. The findings for mechanical integrity of the cement sheath provide an upper bound for its strength. The response of the well system to casing expansion and contraction due to well pressure cycling also provide bounds on the strength of casing-cement-rock interfaces. A combination with well models is needed to constrain these mechanical properties further, and to upscale the scaled-down well system to dimensions of actual wells (e.g., Moghadam et al. 2022; 2023). The advantage is that the current experiments provide data on casing-cement-rock system for a realistic well system configuration, and relevant well stresses and well pressure cycling conditions that are representative of actual wells. Axial and confining stress, well and pore pressure, can, combined with dimensions of casing, cement and sandstone be written in terms of well stresses and upscaled using analytical models (Teodoriu et al. 2010; Agofack and Cerasi 2021). Most other studies investigate individual components of well systems (i.e. casing steel, well cement, or reservoir rock), focus on casing-cement interaction, or apply different stress boundary conditions in laboratory experiments (Skorpa et al. 2018; Stormont et al. 2018; Nasiri et al. 2023; Ugarte et al. 2024, see also the accompanying studies of Corina et al. 2022; 2023 and reviews therein). The data in this study can be combined with data from these studies to compare findings. The combined data can better constrain model input parameters for mechanical behaviour of the sandstone, cement and casing, and, in particular properties of the casing-cement-rock interfaces.

4.3 Limitations of experiments and application to storage sites

As this study addresses overarching topics of durability and integrity of well systems, a discussion on some of the main limitations is warranted. First, interpretation of effects of H_2 exposure and well pressure cycling on system performance would have been easier if standardized experimental protocols could have been used. In the current experiments experimental protocols changed in subsequent experiments. It should be noted that this study is the first that uses the newly developed scaled-down well setup to investigate effects of H_2 exposure and well pressure cycling on system performance. Therefore, the experiments are pilot tests with protocols that needed to be optimized in subsequent experiments.

Second, H_2 exposure in autoclaves and pore pressure cycling using water in a triaxial apparatus is performed sequentially in both studies. With this approach, potential effects of chemical alteration by H_2 exposure on well system properties can be studied by comparing behaviour of scaled-down well systems without exposure and with exposure to N_2 and H_2. A limitation of this approach is that sample variability may potentially also lead to different behaviour of scaled-down well systems in different experiments. Repeated experiments to evaluate reproducibility and disentangle effects of exposure and sample variability were not performed in this study. Focus was on performing very long term experiments so that changes in the behaviour of scaled-down well systems in individual experiments can be picked up. Another limitation of this approach is that well pressure cycling is performed with water in the triaxial experiments and not with H_2 (for safety reasons). Although mechanical boundary conditions (i.e. pressure and stress conditions) are similar for well pressure cycling with water or H_2, chemical effects during cycling may be different. It should be noted that chemical effects on well materials generally occur at longer timescales than mechanical effects, but coupled

chemical, hydrological and mechanical processes that are initiated or enhanced by the presence of water or H_2 are not accounted for in the experiments. Some types of deformation processes are dependent on or enhanced by chemical environments that may be controlled by the presence of H_2, for example stress corrosion cracking (Atkinson and Meredith, 1981; Brantut et al. 2014; Heinemann et al. 2021). As water instead of H_2 is used for pore pressure cycling in this study, the effect of H_2 controlled chemical environment on injectivity and productivity *during well pressure cycling* is not accounted for. In case of stress corrosion cracking, the effect of pore fluid chemistry on sandstone compaction is more pronounced in sandstone saturated with water compared to dry sandstone or sandstone saturated with supercritical or acidic fluids (Schimmel et al. 2022).

Third, despite that total experimental time was considerable due to long term experiments, only limited variations in sandstone type, casing-cement-rock configuration and well pressure cycling protocol could be tested. For example, shallower, less cemented and consolidated sandstones may show much larger inelastic deformation and associated effects of well pressure cycling on the behaviour of the scaled-down well system. Also, the range of applied well pressures during cycles is larger and the duration of pressure cycles (rate of pressure changes) shorter than expected for most storage sites. Therefore, experiments should be regarded as a "worst case scenario" approach. More experiments are needed to evaluate the importance of variations of these factors on the behaviour of well systems.

Fourth, application of results to actual storage sites would require upscaling of experimental results. Experimental results for the scaled-down well system need to be combined with analytical or numerical models to properly upscale and more directly apply results to actual storage well systems. There are good modelling approaches available (e.g., Moghadam et al. 2023), but such analysis is beyond the scope of this study.

Fifth, the focus of this study is mainly on mechanical and fluid flow properties of the scaled-down well system. The effects of H_2 exposure on these properties is investigated but to a limited extent. For example, changes in pore fluid chemistry and rock mineralogy or microstructure have not been performed. Also, microbial reactions may affect these properties, but have not been addressed in this study. Other studies performed within the framework of the HyUSPRe project have addressed these factors in great detail (see www.hyuspre.eu). Results from these studies can be compared to this study to assess the importance of these factors affecting the durability and integrity of well systems.

4.4 Mitigation options for loss of durability and integrity of well systems

The experimental results of this study suggest that the properties and behaviour of components in well systems can sustain long term pressure cycling without loss of integrity, at least for the type of sandstone and conditions investigated (i.e. relatively well-cemented, consolidated Bentheim sandstone at conditions equivalent to reservoir depths up to ~2.5 km). As indicated in section 4.3, other types of sandstone (e.g., less consolidated, poorly cemented sandstone in shallower reservoirs) may be more prone to formation damage and clogging of injection points (Bennion et al. 2002; Zeng et al. 2024). Also, it cannot be excluded that long term cyclic injection and withdrawal of H_2 lead to chemical environments in the near well reservoir that alters the mechanical properties of sandstone so that formation damage occurs.

Formation damage can lead to permeability reduction and loss of injectivity and productivity during H_2 storage operations. Extensive formation damage and associated inelastic strain can also lead to reduced mechanical support of well sections and instabilities. Formation damage in the near well reservoir critically depends on in situ stress conditions as well as on (changes in) reservoir properties. In situ stresses change due to a combination of direct pressure, poro-elastic and thermo-elastic effects (Buijze et al. 2020). In the near well reservoir, direct pressure effects are caused by local changes in pore pressure. Poro-elastic and thermo-elastic effects are caused by reservoir expansion or contraction due to pore pressure or temperature changes. These effects can originate from different parts of the reservoir or extend to a larger reservoir volume. The combination of these effects can also lead to local stress conditions that are prone to hydraulic fracturing. In particular, progressive cooling of the near well reservoir by repeated injection of a relatively cold H_2 gas stream can bring the local stress state closer to fracturing conditions. Note that in this case cooling results from the temperature difference between the H_2 gas stream and reservoir, and not from Joule-Thompson effects as is important for CO_2 injection. Although, hydraulic fracturing could initially enhance reservoir injectivity and productivity, it likely also introduces unstable flow conditions during long term cyclic injection and withdrawal of H_2. The durability of well systems may be negatively impacted if hydraulic fracturing occurs. Accordingly, direct pressure, poro-elastic and thermo-elastic effects on in situ stresses all need to be taken into account to prevent formation damage and hydraulic fracturing.

Mitigation options for loss of durability and integrity of well systems can be outlined in terms of specific prevented and control measures. These measures can be performed as part of risk management procedures (see also, Corina et al. 2022). In planning of storage operations, optimum injection and withdrawal conditions can be determined so that risks of formation damage or hydraulic fracturing are minimized. During storage operations, detailed monitoring of well pressures can be performed to detect changes in reservoir injectivity and productivity that may point to formation damage or hydraulic fracturing. If problematic changes in reservoir injectivity and productivity are detected, H_2 injection and withdrawal conditions can be modified or specific well operations can be attempted to improve injectivity/productivity. If injectivity/productivity persist, different parts of the reservoir can be used for injection and withdrawal of the H_2 gas stream, either by perforating wells at different depth, or, ultimately by drill new storage wells. Of course, feasibility of drilling new wells depend on characteristics of the storage complex and economic factors.

Beside these options, related to prevention or remediation of reservoir injectivity/productivity or mechanical instablilities, more general mitigation options for loss of durability and integrity of well systems can also be considered. Risks associated with well integrity are, in most cases, related to improper placement and cementation. Therefore, proper assessment of the status of all (active and decommisioned) wells is important, in particular in case existing wells are re-used and in case gas production wells are turned into hydrogen storage wells. Ensuring proper cementation of new storage well is also an important focal point for mitigating well integrity issues.

An important note is that most of these mitigation options are similar to those for natural gas storage. If chemical effects on well materials or reservoir properties can be excluded and different properties of natural gas and H_2 gas stream are accounted for, best practices for storage of natural gas are largely also applicable to storage of hydrogen.

5 Summary & conclusions

The durability and integrity of well systems were investigated using a newly developed scaled-down well system at pressures, temperatures and stresses representative of porous sandstone reservoirs at depths up to ~2.5 km. The scaled-down well system consists of a steel casing that is cemented in a hollow porous sandstone reservoir sample. The setup can be viewed as a scaled-down analogue of a cemented (perforated) well section at reservoir level. Two types of well-cemented, consolidated sandstones were tested, Rijswijk White sandstone and Bentheim sandstone. Casings were either fully perforated to hydraulically connect casing and sandstone, partially perforated to hydraulically connect casing to the interface between casing and intact cement sheath, or not perforated to prevent hydraulic connection between cemented sandstone and casing. Intact casings allow effects of casing expansion and contraction to be studied. Class G cement was used to cement the casing in the hollow sandstone sample. The scaled-down well system was placed in a triaxial apparatus to perform long term well pressure cycling at representative axial stresses, confining stresses and temperatures for injection and withdrawal of hydrogen in porous sandstone reservoirs at depth. Experiments of 104-842 hrs duration with 34-454 well pressure cycles of 1, 10 or 100 hrs were performed. Well pressure cycling involved three steps: (1) constant P_w of 10 or 25 MPa for 20, 200 or 2000 minutes, (2) decreasing P_w to 5 or 1 MPa in 20, 200 or 2000 minutes, and (3) increasing P_w to 10 or 25 MPa in 20, 200 or 2000 minutes. Scaled-down well system with fully perforated casings were exposed to N_2 and H_2 in autoclaves to study the effects of H_2 exposure on sandstone injectivity and productivity. Effects of H_2 exposure and well pressure cycling on sandstone injectivity and productivity and on the integrity of the scaled-down well system was investigated by analyzing sandstone pore pressure response and injected or produced fluid volumes, and based on a proxy for injectivity and productivity (IP index).

The main conclusions based on the experimental results are:

- Effects of H_2 exposure and well pressure cycling on sandstone injectivity and productivity or integrity of the scaled-down well systems with perforated casings are small. No major changes in injectivity/productivity or integrity are observed, in particular if similar well pressure cycles at stress conditions of ~2.5 km equivalent reservoir depth are compared.
- Prolonged well pressure cycling at reservoir conditions for scaled-down well systems with perforated casings that have been exposed to H_2 shows a small decrease injectivity and productivity. This effect may be due to inelastic deformation (compaction) and associated changes in mechanical and flow properties of sandstone. For the sandstone tested, the effects are likely too limited to significantly affect H_2 injection and withdrawal operations.
- A marked change in the response of sandstone pore pressure to pressure cycling is only observed for the scaled-down well system with partial perforations and intact cement sheath. Likely, the cement sheath cannot sustain cyclic pressure differences between the casing and sandstone and fracturing of the cement sheath around the perforations initiated hydraulic connection between casing and sandstone. This observation can be used to derive the limit in pressure different for ensuring cement

sheath integrity, but the partially perforated casing is not considered representative for well systems at actual underground hydrogen storage sites.

- Duration of experiments was extensive with a large number of well pressure cycles performed in individual experiments, which provides valuable insights for durability and integrity of storage sites. However, some main limitations for application of results to actual storage sites are that (1) repeated experiments with standardized protocols to test reproducibility were not performed, (2) variations in type of sandstone, configuration of scaled-down well system, and well pressure cycles was limited, and (3) H_2 exposure in autoclaves and pore pressure cycling with water as pore fluid is performed sequentially in both studies which means effects of chemical environment on injectivity/productivity *during* cycling is not accounted for.

Implications for underground hydrogen storage and mitigation options for loss of durability and integrity of well systems have also been addressed:

- Effects of cyclic H_2 injection and withdrawal on sandstone injectivity and productivity are limited for the type of sandstone and conditions tested in the experiments.
- A combination of the experimental results for scaled-down well system with analytical or finite element models of well systems can be used to upscale results to actual storage wells.
- Mitigation options for loss of durability and integrity of well systems that have been discussed are (1) determination of optimum injection and withdrawal conditions that take into account risks of formation damage or hydraulic fracturing, in particular for poorly cemented sandstones, (2) detailed monitoring of well pressures to detect changes in reservoir injectivity and productivity that may point to formation damage or hydraulic fracturing, (3) considering different parts of the reservoir for injection and withdrawal of the H_2 gas stream, either by perforating wells at different depth, or, ultimately by drill new storage wells if severe well integrity issues occur, and (4) perform proper assessment of the status of all (active and decommissioned) wells, in particular in case existing wells are re-used and in case gas production wells are turned into hydrogen storage wells
- Mitigation options that are similar to those for natural gas storage can be adopted if chemical effects on well materials or reservoir properties can be excluded and different properties of natural gas and H_2 gas stream are accounted for.

6 References

Agofack, N. & Cerasi, P. 2021. Numerical simulation of fractures propagation around the wellbore: Effect of the surrounding rock's stiffness. *In:* 55th US Rock Mechanics/Geomechanics Symposium held in Houston, Texas, USA, 20-23 June 2021, ARMA-2021-1233.

Atkinson, B.K., Meredith, P.G. 1981. Stress corrosion cracking of quartz: a note on the influence of chemical environment. *Tectonophysics 77* (1-2), T1-T11, doi.org/10.1016/0040-1951(81)90157-8.

Bennion, D.B. 2002. An overview of formation damage mechanisms causing a reduction in the productivity and injectivity of oil and gas producing formations. *Journal of Canadian Petroleum Technology* 41(11), doi.org/10.2118/02-11-DAS.

Brantut, N., Heap, M. J., Meredith, P. G., & Baud, P. 2013. Time-dependent cracking and brittle creep in crustal rocks: A review. *Journal of Structural Geology* 52, 17–43. doi.org/10.1016/j.jsg.2013.03.007.

Buijze, L., Van Bijsterveldt, L., Cremer, H., Paap, B., Veldkamp, H., Wassing, B., . . . & J. Ter Heege, 2020. Review of induced seismicity in geothermal systems worldwide and implications for geothermal systems in the Netherlands – CORRIGENDUM. *Netherlands Journal of Geosciences* 99 (E10), doi:10.1017/njg.2020.9.

BVEG, 2021. Leitfaden Bohrungsintegrität. Stand:07/2021. *Bundesverband Erdgas, Erdöl und Geoenergie e. V.* Report.

Corina, A., Zikovic, V., Soustelle, V. & Ter Heege, J. 2022: Review of current practices and existing experimental data for well and rock materials under cyclic hydrogen injection and withdrawal, 60 pp, Report Horizon2020 HyUSPRe project.

Corina, A.N., Soustelle, V. & Ter Heege, J.H., 2023. Report with new experimental data on reactions between H2 and well cement and effects on fluid flow and mechanical properties of well cement, 37 pp, Report Horizon2020 HyUSPRe project.

Dabbaghi, E. Ng, K., Brown, T.C., Yu, Y. 2024. Experimental study on the effect of hydrogen on the mechanical properties of hulett sandstone. International Journal of Hydrogen Energy 60, 468-478. doi.org/10.1016/j.ijhydene.2024.02.210.

Dubelaar, C.W. & Nijland, T. G., 2015. The Bentheim Sandstone: geology, petrophysics, varieties and its use as dimension stone. In: Engineering Geology for Society and Territory- Vol. 8 Preservation of cultural heritage, edited by: Lollino, G., Giordan, D., Marunteanu, C., Christaras, B., Yoshinori, I., and Margottini, C., Springer International Publishing, Switzerland, 557–563. doi: 10.1007/978-3-319-09408-3_100.

Gasda, S.E., Bachu, S., Celia, M.A. 2004. Spatial characterization of the location of potentially leaky wells penetrating a deep saline aquifer in a mature sedimentary basin. *Environ Geol. 46*, 707–720. doi.org/10.1007/s00254-004-1073-5.

Haider, M.L. 1937. The productivity index. *Transactions of the AIME* 123 (01), 112–119, doi.org/10.2118/937112-G.

Heinemann, N., Alcalde, J., Miocic, J. M., Hangx, S. J. T., Kallmeyer, J., Ostertag-Henning, C., Hassanpouryouzband, A., Thaysen, E. M., Strobel, G. J., Schmidt-Hattenberger, C., Edlmann, K., Wilkinson, M., Bentham, M., Stuart Haszeldine, R., Carbonell, R., & Rudloff, A. 2021. Enabling large-scale hydrogen storage in porous media – the scientific challenges. *Energy & Environmental Science 14*(2), 853-864, doi.org/10.1039/d0ee03536j.

Moghadam, A., K. Castelein, J. ter Heege & B. Orlic, 2022. A study on the hydraulic aperture of microannuli at the casing–cement interface using a large-scale laboratory setup. *Geomechanics for Energy and the Environment* 29, 100269, doi.org/10.1016/j.gete.2021.100269.

Moghadam, A., Peters, E., Nelskamp, S. 2023. Gas leakage from abandoned wells: A case study for the Groningen field in the Netherlands, International Journal of Greenhouse Gas Control 126, 103906, doi.org/10.1016/j.ijggc.2023.103906.

Naderloo, M. Kumar, K.R., Hernandez, E., Hajibeygi, H., Barnhoorn, A. 2023. Experimental and numerical investigation of sandstone deformation under cycling loading relevant for underground energy storage. *Journal of Energy Storage* 64, 107198, doi.org/10.1016/j.est.2023.107198.

Nasiri, A., Ravi, K., Prohaska-Marchried, M., Feichter, M., Raith, J., Coti, C., Baronio, E., Busollo, C., Mantegazzi, A., Pozzovivo, V., & S. Pruno. 2023. An Interdisciplinary Approach to Investigate the Cement Integrity for Underground Hydrogen Storage Wells. *In*: SPE EuropEC - Europe Energy Conference featured at the 84th EAGE Annual Conference & Exhibition, Vienna, Austria, June 2023, doi.org/10.2118/214423-MS.

Soustelle, V., Van Winden, J., Houben, M., 2023. Experimental data on reactions between hydrogen and rock samples from reservoir and geological seals and effects on fluid flow and mechanical properties of reservoir and caprock, 66 pp, Report Horizon2020 HyUSPRe project.

Schimmel, M. T. W., Hangx, S. J. T., & Spiers, C. J. 2021. Impact of Chemical Environment on Compaction Behaviour of Quartz Sands during Stress-Cycling. *Rock Mechanics and Rock Engineering 54* (3), 981-1003. doi.org/10.1007/s00603-020-02267-0.

Skorpa, R., Øia, T., Taghipour, A. & Vrålstad, T. 2018. Laboratory Set-Up for Determination of Cement Sheath Integrity During Pressure Cycling. *Proceedings of the ASME 2018 37th International Conference on Ocean, Offshore and Arctic Engineering* 8: Polar and Arctic Sciences and Technology; Petroleum Technology. Madrid, Spain. June 17–22, 2018. ASME. doi.org/10.1115/OMAE2018-78696.

Stormont, J.C., Fernandez, S.G., Taha, M.R., Matteo, E.N. 2018. Gas flow through cement-casing microannuli under varying stress conditions. Geomechanics for the Energy and the Environment 13, 1-13, doi.org/10.1016/j.gete.2017.12.001.

Teodoriu, C., I. Ugwu & J. Schubert. 2010. Estimation of casing-cement-formation interaction using new analytical model. *In*: *Proceedings of the SPE EUROPEC/EAGE Annual conference, 14-17 June 2010*. SPE 131335.

Ugarte, E.R., Tetteh, D. Salehi, S. 2024. Experimental studies of well integrity in cementing during underground hydrogen storage. *International Journal of Hydrogen Energy* 51 Part D, 473-488, doi.org/10.1016/j.ijhydene.2023.07.037.

Zeng, L., Sander, R., Chen, Y., Xie, Q. 2024. Hydrogen Storage Performance During Underground Hydrogen Storage in Depleted Gas Reservoirs: A Review, *Engineering* in press, doi.org/10.1016/j.eng.2024.03.011.

Appendix A: Sample photos

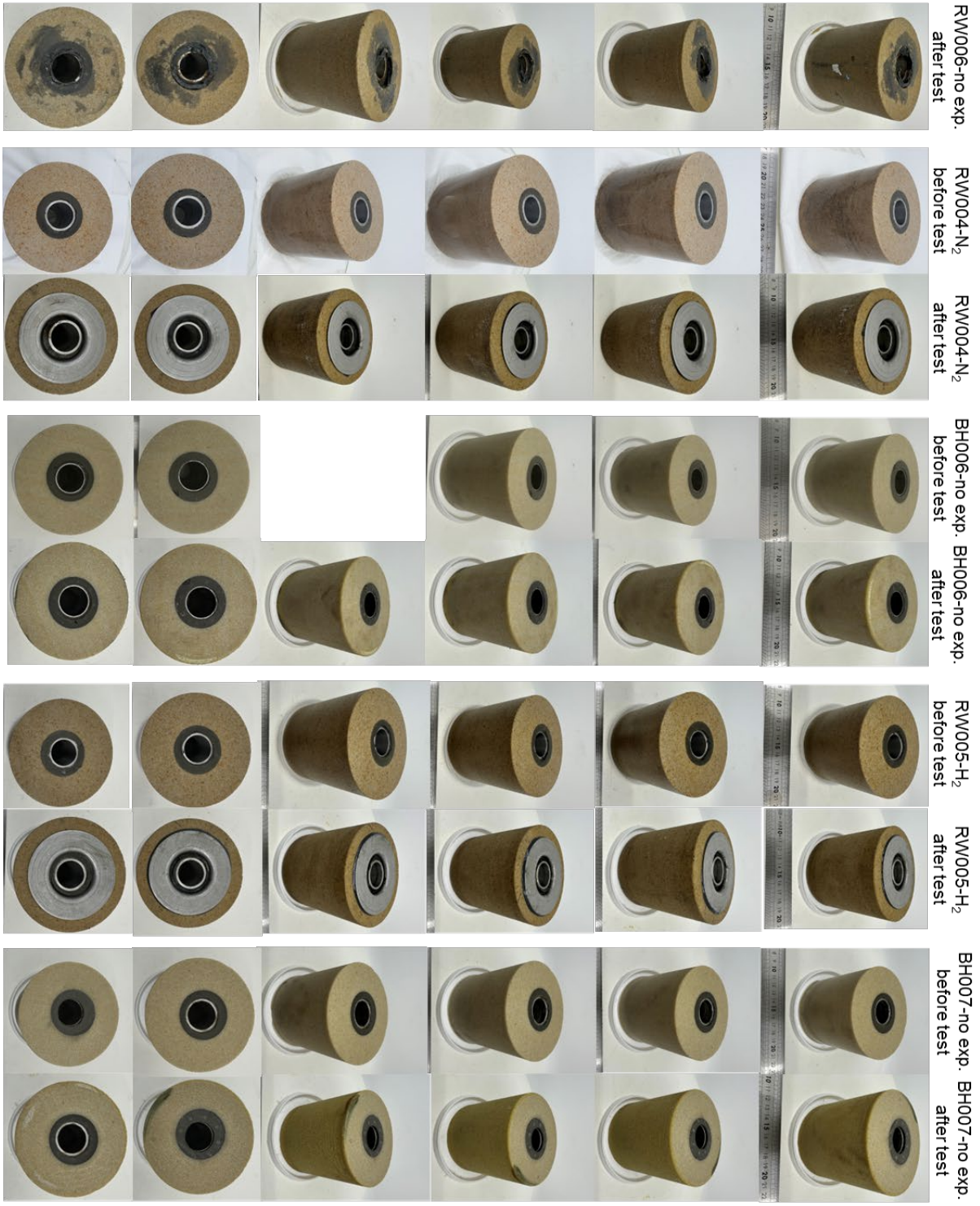

Figure A-1. Sample photos of all samples tested in experiments SDW002-SDW006 before and after the experiments (cf. Table 2-2). Rows show bird's eye views, top and bottom of sample. RW- Rijswijk White sandstone, BH- Bentheim sandstone, no exp.- not exposed after cement curing, N_2- exposed to N_2 in autoclaves after cement curing, H_2- exposed to H_2 in autoclaves after cement curing.

Appendix B: Experimental data (larger figures)

B.1 SDW002_RW006

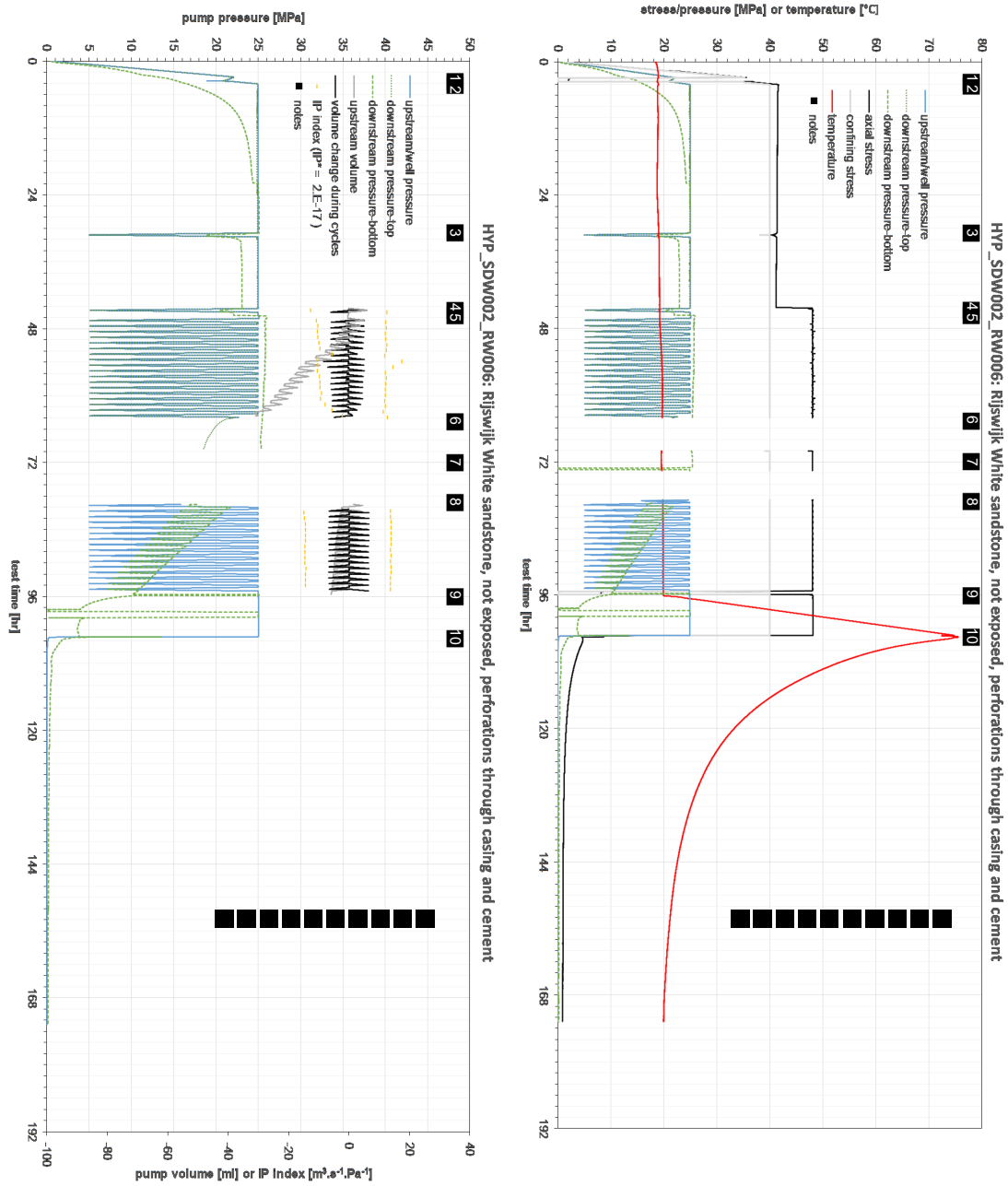

Figure B-1. Experimental conditions and well pressure cycles for experiment SDW002 on Rijswijk White sandstone (SDW002_RW006, no exposure, tested after cement curing). (a) Axial and confining stress, well, upstream and downstream pressure (as measured by pressure sensors in between pressure pumps and sample), and temperature. (b) well, upstream and downstream pressure and volume (as measured by pressure pumps), and calculated volume changes for each pressure cycle and IP index (injectivity/productivity proxy, cf. section 2.6). Notes of critical experimental steps are also indicated.

B.2 SDW003_RW004-N_2

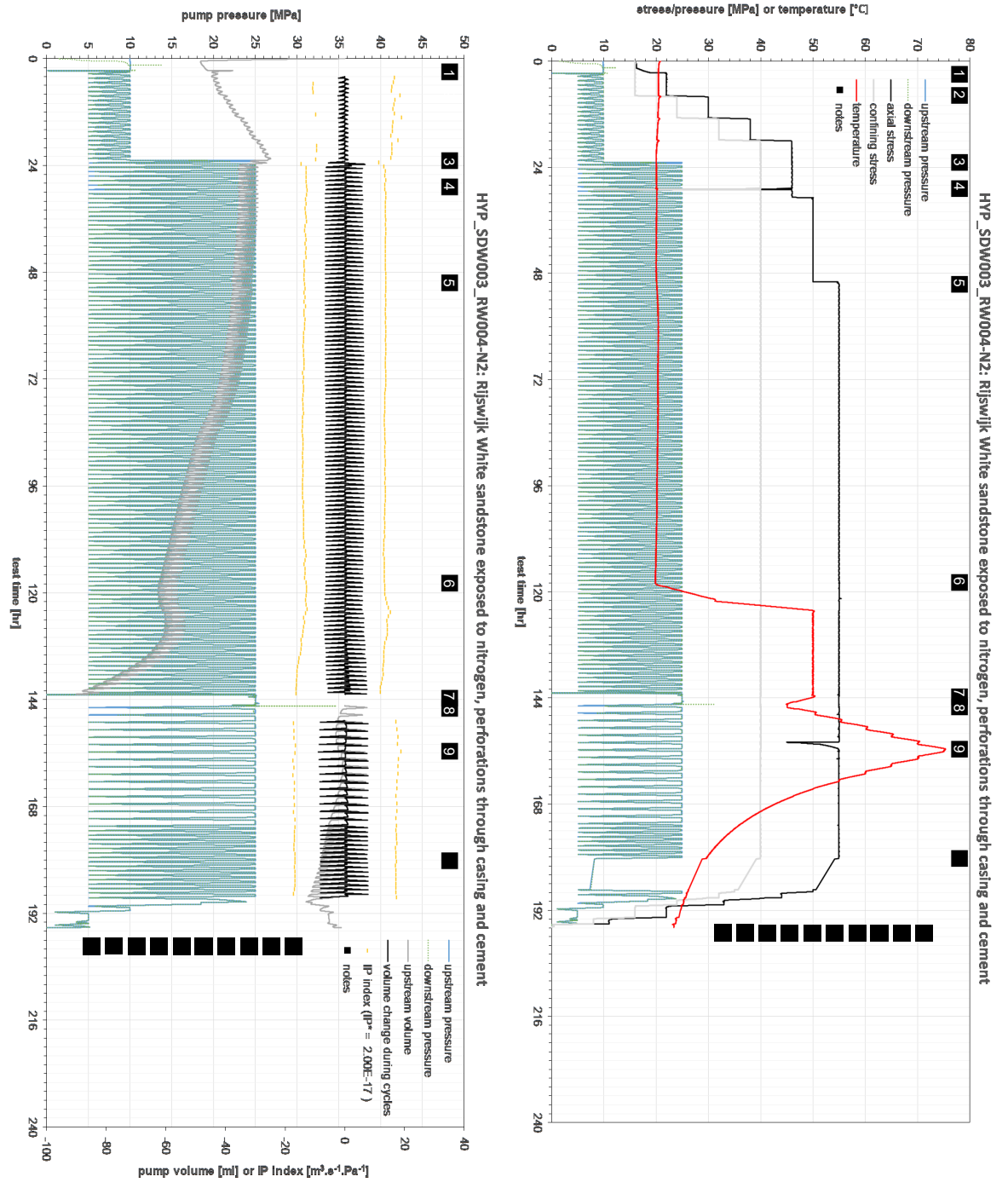

Figure B-2. Experimental conditions and well pressure cycles for experiment SDW003 on Rijswijk White sandstone (SDW003_RW004, N_2 exposure for ~143 days at ~19 MPa and 80°C). (a) Axial and confining stress, well, upstream and downstream pressure (as measured by pressure sensors in between pressure pumps and sample), and temperature. (b) well, upstream and downstream pressure and volume (as measured by pressure pumps), and calculated volume changes for each pressure cycle and IP index (injectivity/productivity proxy, cf. section 2.6). Notes of critical experimental steps are also indicated.

B.3 SDW005_RW005-H_2

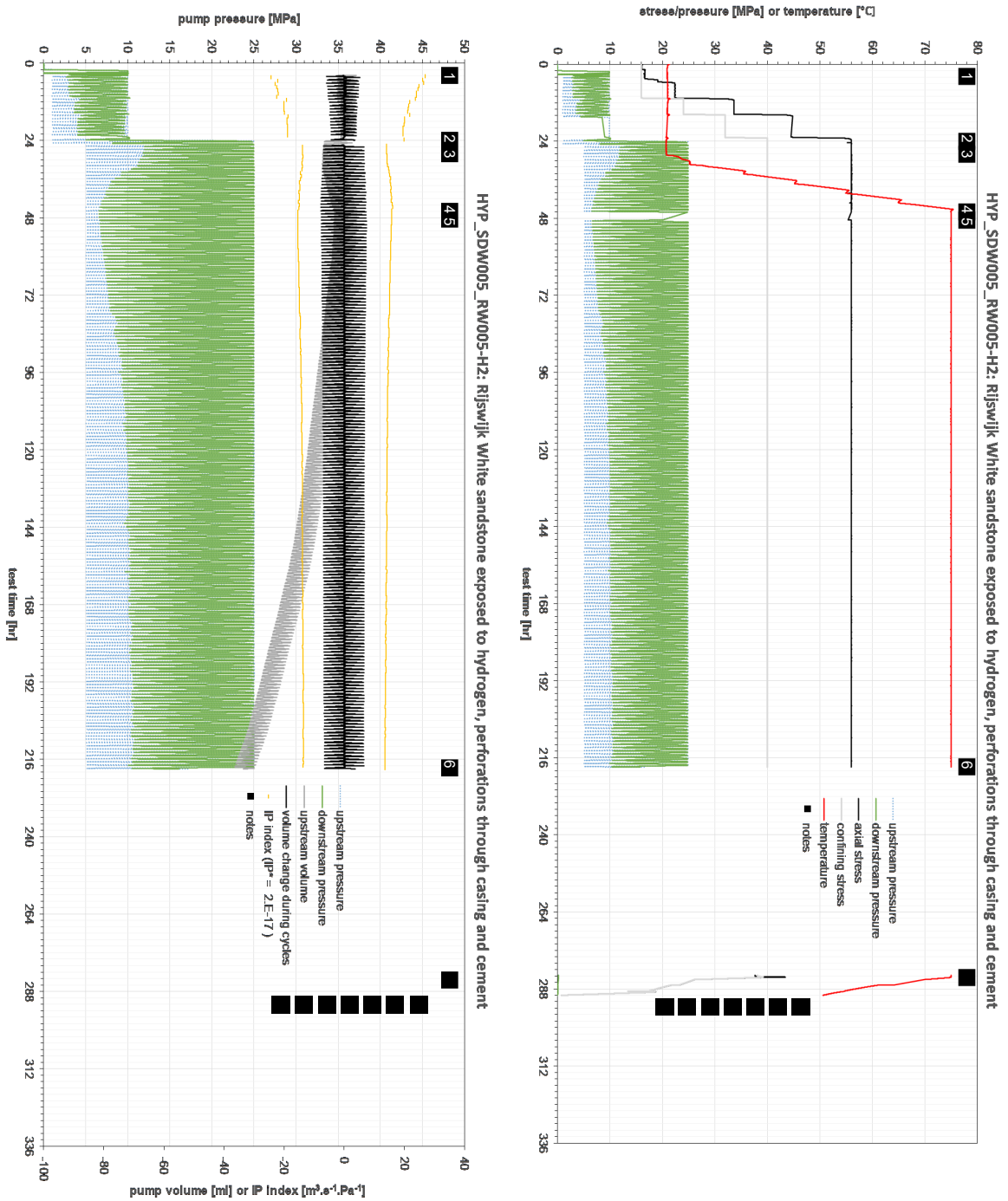

Figure B-3. Experimental conditions and well pressure cycles for experiment SDW005 on Rijswijk White sandstone (SDW005_RW005, H_2 exposure for ~143 days at ~19 MPa and 80°C). (a) Axial and confining stress, well, upstream and downstream pressure (as measured by pressure sensors in between pressure pumps and sample), and temperature. (b) well, upstream and downstream pressure and volume (as measured by pressure pumps), and calculated volume changes for each pressure cycle and IP index (injectivity/productivity proxy, cf. section 2.6). Notes of critical experimental steps are also indicated.

B.4 SDW004_BH006

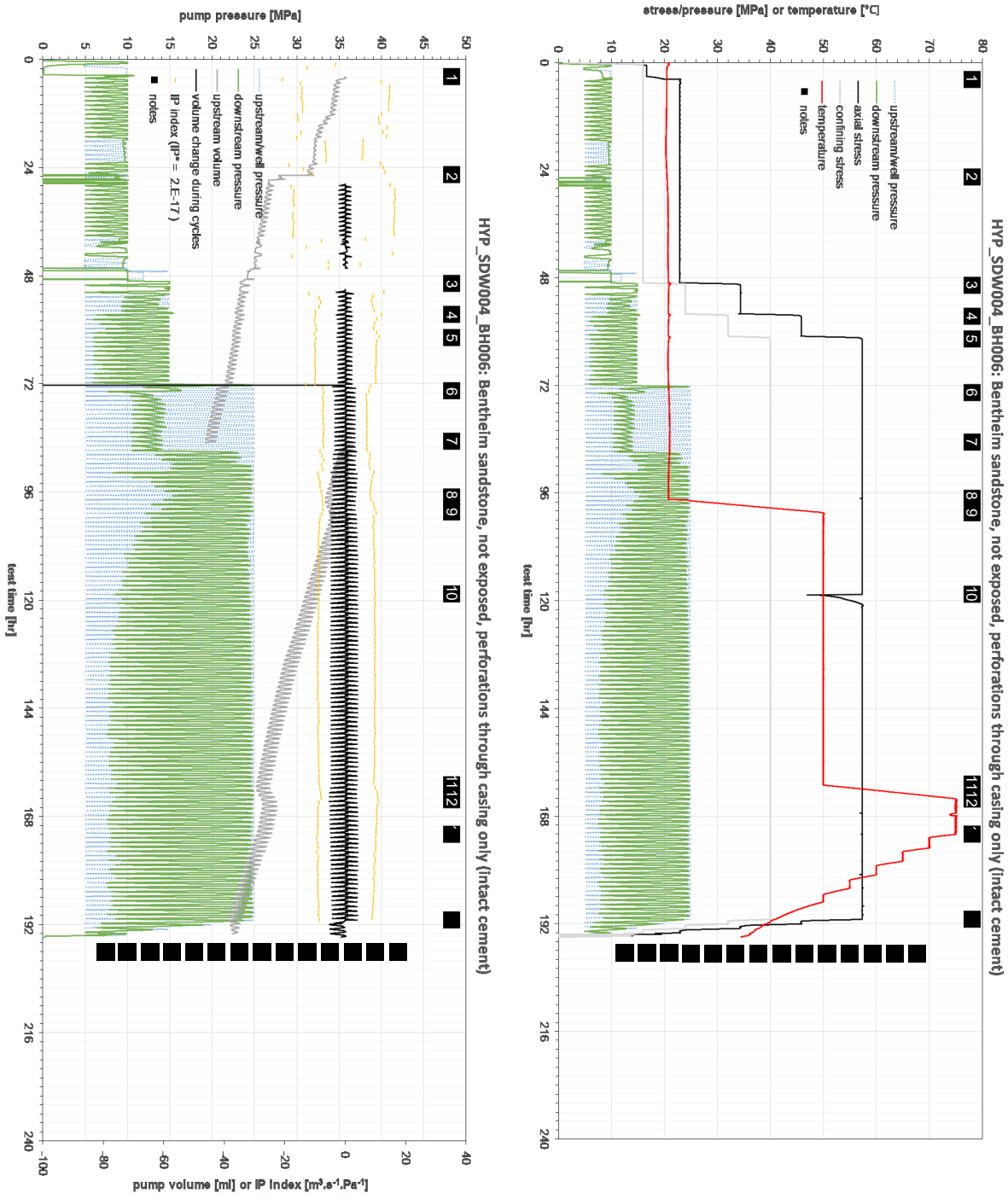

Figure B-4. Experimental conditions and well pressure cycles for experiment SDW004 on Bentheim sandstone (SDW004_BH006, no exposure, tested after cement curing). (a) Axial and confining stress, well, upstream and downstream pressure (as measured by pressure sensors in between pressure pumps and sample), and temperature. (b) well, upstream and downstream pressure and volume (as measured by pressure pumps), and calculated volume changes for each pressure cycle and IP index (injectivity/productivity proxy, cf. section 2.6). Notes of critical experimental steps are also indicated.

B.5 SDW006_BH007

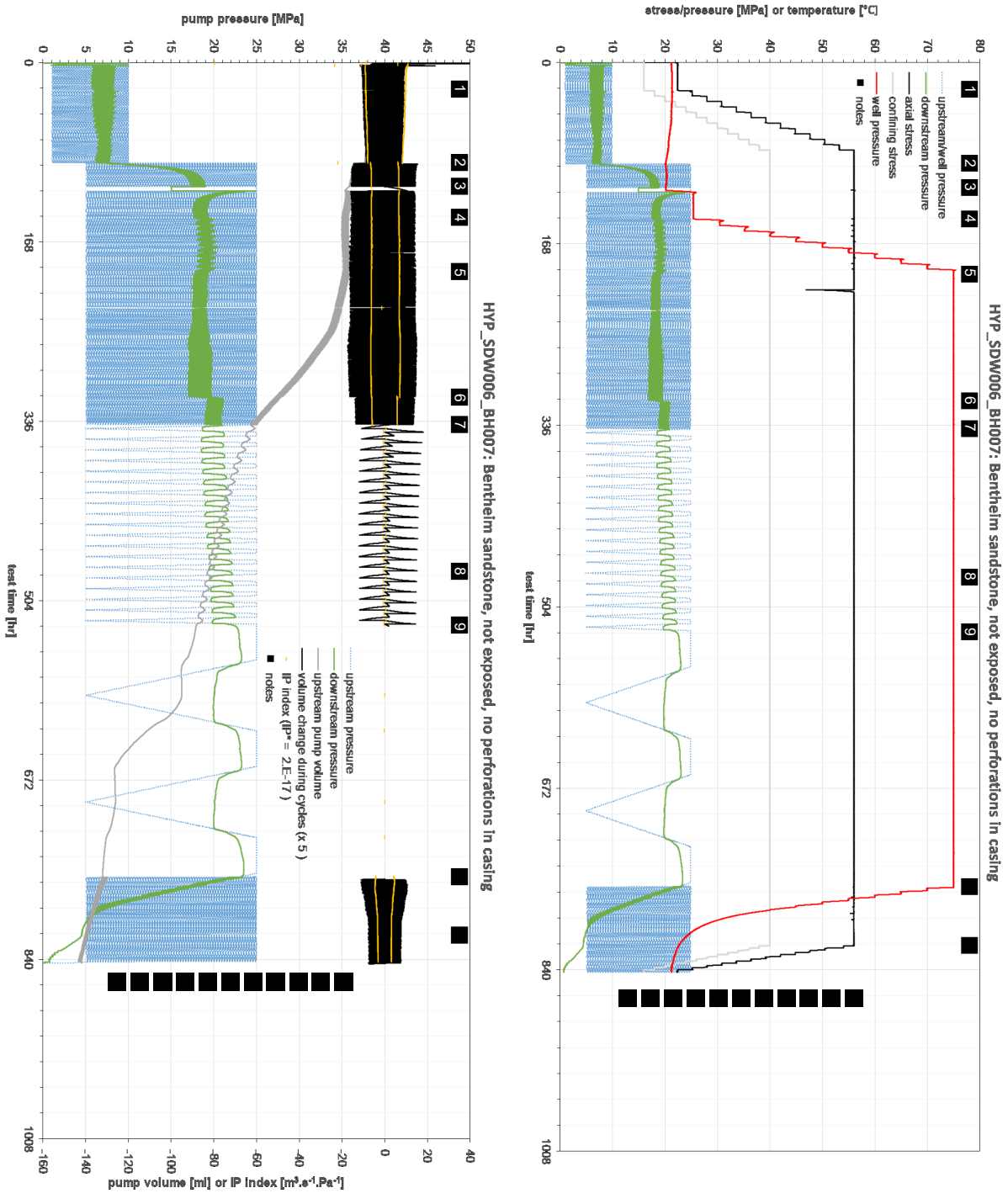

Figure B-5. Experimental conditions and well pressure cycles for experiment SDW006 on Bentheim sandstone (SDW006_BH007, no exposure, tested after cement curing). (a) Axial and confining stress, well, upstream and downstream pressure (as measured by pressure sensors in between pressure pumps and sample), and temperature. (b) well, upstream and downstream pressure and volume (as measured by pressure pumps), and calculated volume changes for each pressure cycle and IP index (injectivity/productivity proxy, cf. section 2.6). Notes of critical experimental steps are also indicated.